A MICROSPHERE BASED MICROFLUIDIC CHECK VALVE

by

Kevin Ou

B.Eng.Mgt, McMaster University, 2009

A THESIS SUBMITTED IN PARTIAL FULFILLMENT OF

THE REQUIREMENTS FOR THE DEGREE OF

MASTER OF APPLIED SCIENCE

in

THE FACULTY OF GRADUATE STUDIES

(Mechanical Engineering)

THE UNIVERSITY OF BRITISH COLUMBIA

(Vancouver)

September 2011

Abstract

Biomedical applications of Micro-Electro-Mechanical System (MEMS) technology have sprung growth in the field of microfluidic systems and have been attracting much attention from scientific researchers and industry. Implantable drug delivery devices can deliver localized dosage which can reduce the side effects of medication. Such devices can maintain therapeutic concentrations of the drug over extended periods by providing small doses minimizing the risk of systemic toxicity.

Recently, ocular drug delivery devices with micropumps using check valves have been demonstrated. The use of external magnetic actuation in a MEMS-based drug delivery device has been verified in reciprocating diaphragm micropumps. However, the magnetic diaphragm generates low pressures resulting in low flow rates (Re<1).

This work investigates the use of polystyrene (PS) microspheres as resistive elements in a fluidic channel to create a check valve. The check valve takes advantage of the low profile microsphere and flow channel to rectify flow in low pressure and low flow applications. This makes the check valve ideal for thin planar reciprocating micropumps, which can be used as ocular drug delivery devices, with the conjunctival cul-de-sac being a possible site of implantation. The microspheres form a porous media which acts as variable fluid resistors based on the direction of flow, and also increases tortuosity in the check valve limiting diffusion from the device. Three check valve designs were characterized based on their flow rate and diodicity (ratio of flow in the forward and reverse direction). Pump performance, based on the check valves integrated in series with a deflecting diaphragm actuator, was

investigated. Finally, a proof-of-concept diffusion study was conducted using docetaxel (DTX), a low aqueous solubility drug used to treat late stage proliferative retinopathy, as the sample drug to demonstrate the microsphere check valve's ability to limit diffusion from the micropump.

Preface

The work presented in this thesis is based on a manuscript which will be submitted to a journal. A version of the data presented in chapter 3 has been published in:

- K. Ou, M.Chiao, "A Passive Check Valve Using Microspheres for Low Pressure and Low Flow Rate Applications", *The 16th International Conference on Solid-State Sensors, Actuators and Microsystems (TRANSDUCERS 2011)*, Beijing, China, June 5-9, 2011.

I was responsible for all aspects of the work which included, but not limited to, device design, device fabrication and testing, data analysis and manuscript preparation. This includes all work done on the check valve, micropump and trial drug diffusion study. Mr. John Jackson provided technical advice, training on drug release measurement equipment, and helped prepare solutions used in the trial drug diffusion study.

Table of contents

List of tables

List of figures

List of symbols

MEMS	Micro-electro-mechanical system
µTAS	Micrototal analysis systems
µL	Microlitre
nL	Nanolitre
pL	Picolitre
min	Minute
kPa	Kilopascal
Pa	Pascal
Re	Reynolds number
µm	Micrometre
PS	Polystyrene
DTX	Docetaxel
PDMS	Polydimethylsiloxane
Ø	Diameter
°	Degrees
W	Channel width
W_R	Channel width in reverse direction
W_F	Channel width in forward direction
L	Porous media length
L_R	Porous media length in reverse direction
L_F	Porous media length in forward direction
R_{fluid}	Fluidic resistance
Q	Flow rate
P	Pressure
µ	Dynamic viscosity
Ɛ	Porosity
d_p	Diameter of particle or microsphere
A	Cross sectional area
C	Constant

mm	Millimetre
UV	Ultraviolet
°C	Celsius
s	Seconds
cm	Centimeter
RPM	Revolutions per minute
MFCS	Microfluidic control system
ID	Inner diameter
v/v	Volume to volume ratio
F_D	Viscous drag force
U	Mean flow velocity
mg	Milligram
mL	Millilitre
DCM	Dichloromethane
µg	Microgram
w/v	Weight to volume ratio
BSA	Bovine serum albumin
PBS	Phosphate buffered saline
n	Number of samples
H	Channel height
DPM	Disintegrations per minute

Acknowledgements

First and foremost I want to thank my supervisor Dr. Mu Chiao for his guidance, support and friendship. One could not wish for a more patient and caring supervisor.

My sincere thanks go to Dr. Boris Stoeber, Dr. Hongshen Ma, and Dr. Karen Cheung, for their guidance, support, and sharing of laboratory facilities to make this project possible.

It was an honor for me to work with Nazly Pirmoradi, Hadi Mansoor, Farzad Khademolhosseini, and Jacob Yeh in MEMS Lab and members of BioMEMS and Multi-scale Design Lab. I want to thank my friends for their valuable discussions, support and friendship.

Finally, I owe my deepest gratitude to my family and girlfriend Lily for their unconditional love and moral support.

To my parents

Chapter 1: **Introduction**

Advances in Micro-Electro-Mechanical System (MEMS) research have focused on developing miniaturized mechanical and electrical systems using microfabrication techniques. Biomedical applications of MEMS technology have sprung growth in the field of microfluidic systems attracting much attention from scientific researchers and industry [1]. Companies producing medical products are especially interested in microfluidic systems due to their potential biomedical applications which include: micrototal analysis systems (μTAS) [2, 3], point of care diagnostics [4, 5], and drug delivery devices [6-8]. Microfluidics enables the precise manipulation of fluids in small volumes, typically in the μL, nL, and pL scale. The fundamental elements in microfluidics are micropumps, which are relied upon to deliver small fluid volumes in a precise, accurate and reliable manner.

Precise and accurate control of small fluid volumes can greatly benefit drug delivery devices as dosing levels can be finely controlled. Furthermore, implantable drug delivery devices can deliver localized dosage which can reduce the side effects of medication. Such devices can maintain therapeutic concentrations of the drug over extended periods by providing small doses minimizing the risk of systemic toxicity [9]. However, micropumps which can be used in implantable drug delivery devices require unique design considerations.

1.1 Target application in drug delivery

For ophthalmology applications, topical drugs, most commonly in the form of eye drops, are used. However, only 1% to 7% of the drug reaches the target site with the remaining drug

being drained away and systemically absorbed [10, 11]. It is hypothesized that reducing the delivered volume to 5-15 μL at each delivery cycle would limit the drug drainage from the eye [12]. A potential solution is placing a micropump in the conjunctival cul-de-sac. A micropump would draw fluid in the form of tears from the surrounding environment, diffuse with concentrated drug and deliver drug dosage to the eye. Under normal conditions the estimated volume of tears in the conjuctival cul-de-sac is between 7 to 9 μL. Furthermore, the turnover rate of tear fluid is between 0.5 to 2.2 μL min^{-1} and the maximum fluid volume in the conjunctival cul-de-sac is 30 μL [13]. Micropumps are capable of delivering volumes within the physiological range thereby minimizing drug drainage from the eye.

Recently, ocular drug delivery devices with micropumps using check valves have been demonstrated, but they require relatively high working pressures ~10.1 kPa with some devices requiring refills and electrical power [14, 15]. Micropumps which require electrical power as its source of activation energy typically need on-chip batteries or external power for the drug delivery device to be implantable. On-chip batteries may dominate the size of the device and are a major challenge in miniaturization. There is ongoing research in generating electricity from microbial fuel cells [16-18] and other implantable batteries [19], however, their current suitability for powering implantable ocular drug delivery systems continues to be a challenge. One method of bypassing this challenge is to use external actuation, such as magnetic force, to generate flow in the micropump. The use of external magnetic actuation in a MEMS-based drug delivery device has been demonstrated in reciprocating micropumps [20, 21]. However, the magnetic actuator in the form of a magnetic diaphragm generates low pressures resulting in low flow rates ($Re<1$) [22, 23].

1.2 Microvalves

Microvalves play an essential role in micropumps. Active microvalves are not typically used in micropumps since they are essentially small actuators which use mechanical, non-mechanical, and external systems to close off or modify fluid flow. Reciprocating micropumps usually integrate passive valves at the inlet and outlet to control fluid flow; passive valves are generally referred to as check valves [24]. Check valves in the form of cantilever type flaps, membranes, and spherical balls act as fluid diodes in a reciprocating micropump to rectify flow in one direction [25]. Currently, no structurally thin check valve performs well under low pressure and low flow rates. Thin planar check valves with cantilever features allow fluid to in the forward direction while inhibiting flow in the reverse direction by exploiting elastic material compliance [26, 27]. Forward flow is the intended direction of flow and reverse flow is considered leakage in the check valve. The asymmetry ratio of forward flow to reverse flow is defined as diodicity. Loverich et al. developed a micropump with a planar check valve which achieved a maximum diodicity of 3.9 at a flow rate of 15μL min^{-1} [28]. However, these planar check valves require high pressures in the tens of kPa. Diffuser valves with no moving parts have been studied for use in thin planar micropumps; however, they have low diodicity (~1.2) and requires moderate flow rates (Re>20) [29, 30]. Although single millimeter spheres have been used as ball valves in a high pressure millimeter scale check valve pump [31, 32], using many microspheres in a check valve for low pressure, low flow applications have not been studied.

1.3 Research objective

For ocular drug delivery applications, the desired design characteristics of check valve system are: (1) structurally thin (~300-500 μm), with the lower conjunctiva cul-de-sac (Figure 1.1) being a possible site of implantation, (2) the valve can work with low pressure (<1 kPa) generated by the pump, and (3) the check valve exhibits high diodicity (ratio of flow in the forward and reverse direction) and limits diffusion. The goal of this project is to develop a check valve system which can operate to the above specifications.

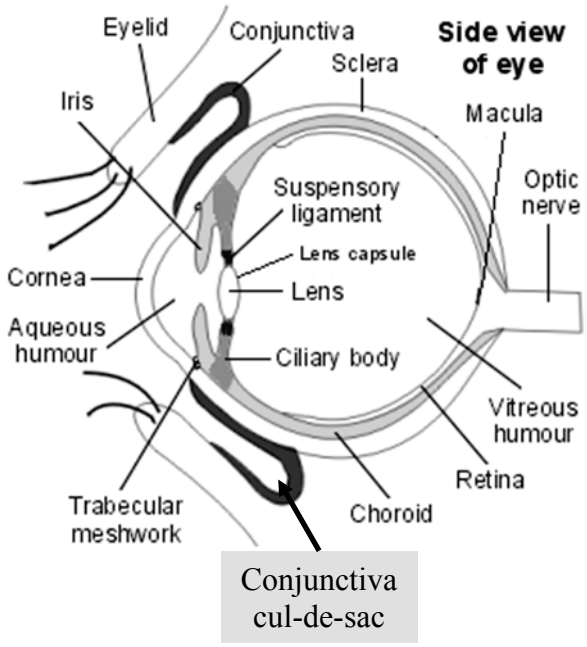

Figure 1.1 A side view of a human eye. The conjunctiva cul-de-sac is possible site of implantation for the drug delivery system [33].

The short term research objective is to investigate the use of polystyrene (PS) microspheres as resistive elements in a fluidic channel to create a thin check valve. The low profile of the microsphere and the flow channel makes the check valve ideal for thin planar reciprocating

micropumps. A second objective is to investigate the performance of a pump configuration, which integrates the check valves in series with a deflecting diaphragm actuator.

Another short term goal of this research project is to demonstrate the microsphere check valve's ability to limit drug diffusion from the micropump by increasing path length and number of curves which drug particles need to travel. This increased diffusion resistance is known as the tortuosity in the system. A proof-of-concept drug delivery study will be conducted on the micropump using docetaxel (DTX), a low aqueous solubility taxane drug, as the sample drug. The use of taxane compounds to treat late stage proliferative retinopathy has been recently proposed [34].

The long-term goal of this project is to develop a MEMS based drug delivery device for ocular applications. Previously, a polydimethylsiloxane (PDMS) based magnetic drug delivery device consisting of a magnetic membrane and a drug reservoir has been developed [21, 35]. The drug delivery will be accomplished by magnetically actuating the membrane to squeeze drug out from the reservoir through an aperture. Since the reported system has no integrated valves, drug diffusion from the aperture is an issue when there is no actuation. The integration of the microsphere check valve with the PDMS magnetic membrane and drug reservoir would allow for remotely controlled ocular drug delivery.

1.4 Thesis organization

In chapter 1 the application of microfluidics to control small volume of fluid using microvalves and micropumps is introduced. In addition, the design requirements, short term and long term research objectives are described.

In chapter 2 the design concept and fabrication method is presented. Theory behind the working principle of the microsphere check valve is explained. Finally, the experimental setup used to characterize the check valve and micropump is presented.

In chapter 3 the experimental results and discussion of the microsphere check valve are presented.

In chapter 4 volume flow from a pneumatically actuated micropump is presented. A trial drug delivery study describes the check valve's ability to limit diffusion from the system.

Finally, conclusions from this research thesis along with recommendations for future work are presented in chapter 5.

Chapter 2: **Methods and materials**

2.1 Design

The check valve is designed to be structurally thin and behave as a fluid diode under low pressure differences to enable pumping under low actuation pressures. The check valve has a channel height of 35 μm and uses Ø20 μm polystyrene (PS) microspheres in the valve chamber. Figure 2.1 shows the top view of the valve chamber. The valve chamber uses two sets of small square pillars with edges aligned 45° to the channel wall to confine the PS microspheres. The square shaped PDMS pillars have a diagonal dimension of 40 μm with and are separated by 10 μm gaps. Larger Ø100 μm circular pillars are used as structural supports to prevent channel collapse. The valve chamber has a reverse channel width W_R in the reverse flow direction (to the left), and a forward channel width W_F in the forward flow direction (to the right). The channel width transitions from the reverse channel width to the forward channel at an angle of 45° relative to the horizontal channel wall. The detailed drawings for the three check valve designs can be found in Appendix A.

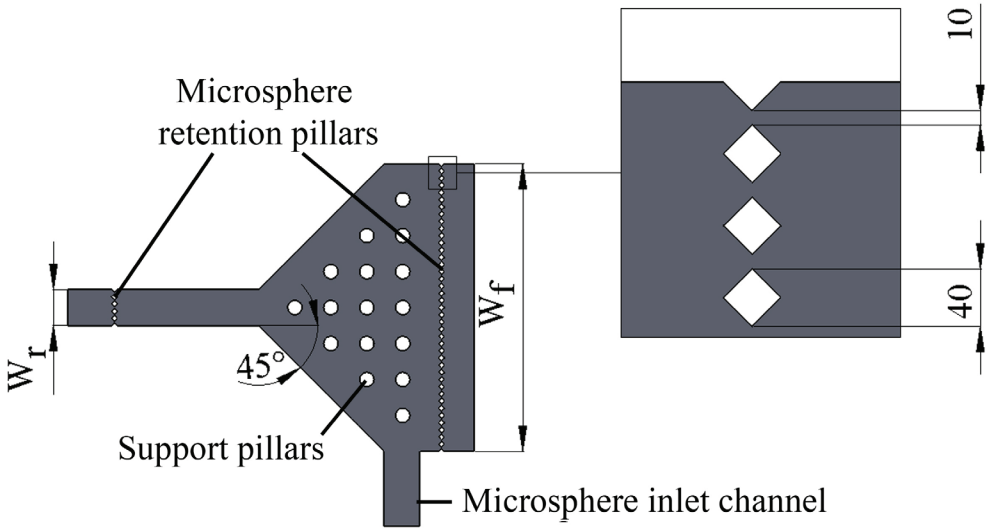

Figure 2.1 Design of valve with narrow channel designated W_R and wide channel designated W_F (dimensions in µm)

A schematic of a reciprocating check valve pump is shown in Figure 2.2 (a). A flexible diaphragm seals a pump chamber, and creates a stroke volume when deflected. Although deflections generated magnetically using a magnetic diaphragm has been reported [22, 23], for simplicity, the diaphragm in this study was deflected using pneumatic pressure induced by a control channel.

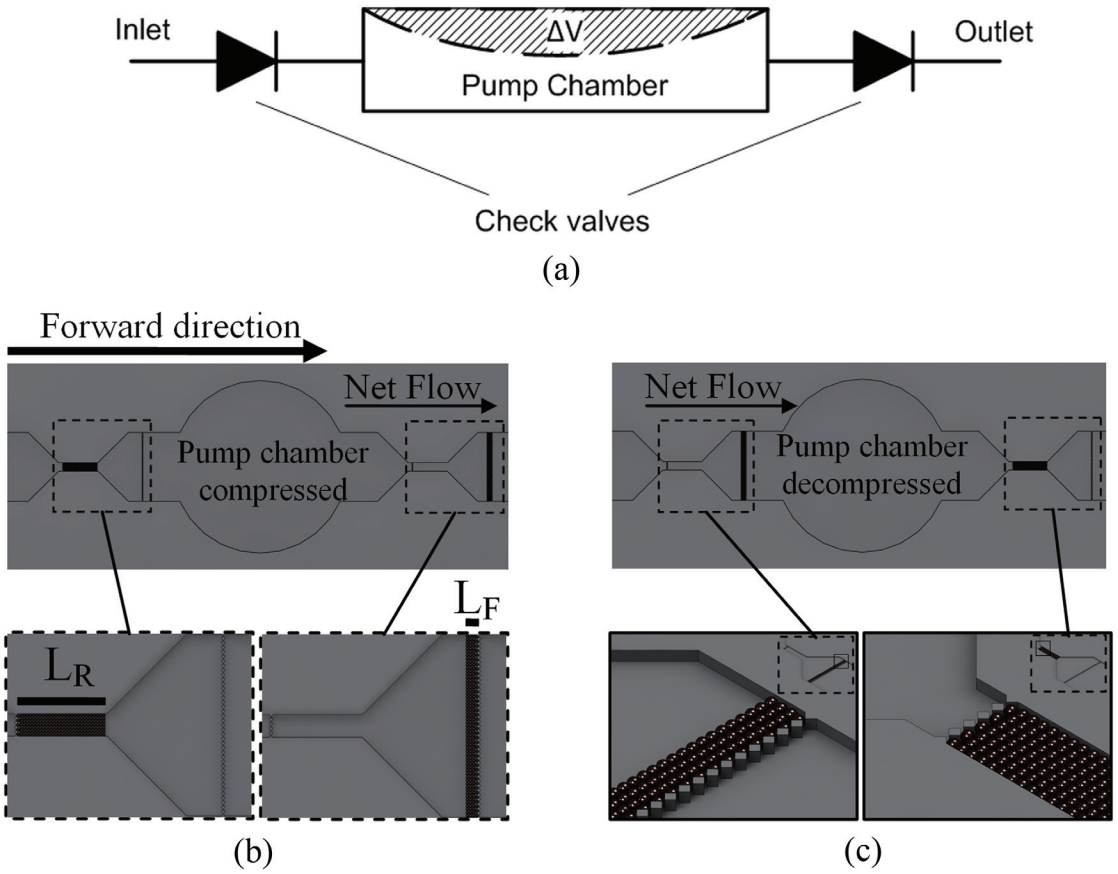

Figure 2.2 (a) Schematic of a pump with check valves at the inlet and outlet side of the reciprocating pump chamber; (b) Top view of the check valve pump showing microsphere position in inlet and outlet side of the valve chambers as the pump diaphragm compresses. Microspheres collect in reverse flow direction for the inlet side valve and collect in the forward flow direction for the outlet side valve; (c) Isometric view of pillars and microspheres in check valve when the pump chamber decompresses

The top view of the check valve and pumping chamber is illustrated in Figure 2.2 (b) and (c). PS microspheres flow freely in the valve chamber moving with the flowing fluid. The flexible diaphragm is in its equilibrium position at the start of the pumping cycle. When an actuation force is applied, the pump chamber is compressed to its minimum volume and the

resulting fluid flow forces microspheres away from the pump chamber illustrated in Figure 2.2 (b).

The length of microsphere packing (*porous media length*) changes due to geometric effects in the check valve chamber as the diaphragm compresses and decompresses. The porous media lengths are represented as L_R and L_F respectively. With high resistance in the inlet check valve and low resistance in the outlet check valve a net flow out of the pump chamber through the outlet check valve is generated. When the actuation force is removed, the diaphragm returns to its equilibrium position, and causes microspheres to move towards the pump chamber shown in Figure 2.2 (c). With high resistance in the outlet check valve and low resistance in the inlet check valve there is a net flow into the pump chamber. The two step pump cycle is summarized in Table 2.1.

Table 2.1 Summary of check valve resistance behavior given $L_R > L_F$ and $R_{fluid} \propto L$. Fluid flows in the path and through the valve of least resistance

	Length of microspheres			
Pump Chamber	Inlet side valve	Outlet side valve	Valve with higher resistance	Resultant flow
Compressed	L_R	L_F	Inlet side	Out through outlet valve
Decompressed	L_F	L_R	Outlet side	In through inlet valve

Three check valve designs based on the ratio of the reverse channel width, W_R, to forward channel width, W_F, (herein described as reverse-forward dimension) were made. The dimension ratios of the three check valves were 250-500 μm, 500-1000 μm, and 250-2000 μm.

Based on the Blake-Kozeny theory of flow through porous media [36], the fluid resistance R_{fluid} is defined in Eq (1) and Eq (2):

$$Q = \frac{\Delta P}{R_{fluid}} \tag{1}$$

$$R_{fluid} = \frac{150\mu}{d_p^2}\frac{(1-\varepsilon)^2}{\varepsilon^3}\frac{L}{A} \tag{2}$$

where flow rate is Q, pressure difference is ΔP, cross-section area of flow though porous media is A, microsphere diameter is d_p, fluid viscosity is μ, and porosity (or void fraction) is ε. A simple assumption of constant microsphere diameter and constant porosity of the porous media suggests that the fluid resistance is linearly proportional to the porous media length and inversely proportional to the cross section area of flow through the porous media. Therefore, the fluid resistance relative to the direction of flow is described by Eq. (3),

$$R_{fluid,direction} = C\frac{L_{direction}}{A_{direction}} \tag{3}$$

$$A_{direction} = W_{direction}\ H \tag{4}$$

where C is a constant based on the porosity, fluid viscosity and diameter of the sphere. Eq (4) calculates the cross section area of flow through the porous media $A_{direction}$ with channel width $W_{direction}$ and channel height H. It should be noted that the channel height remains constant and does not change based on the direction of flow. Under the assumption of constant porosity, the projected area is constant for a fixed number of microspheres forms as described by,

$$\text{Projected area} = \mathrm{W} \times \mathrm{L} = \text{Constant} \tag{5}$$

$$\therefore \mathrm{W_R L_R} = \mathrm{W_F L_F} \tag{6}$$

where W and L are designated channel width and porous media length respectively. Thus, the porous media length in the reverse direction channel (L_R) is W_F/W_R times longer than the porous media length in the forward direction channel (L_F) due to the channel width ratios. Combining Eq (1) to (6) a theoretical diodicity for the microsphere check valve can be calculated using Eq (7).

$$\text{Diodicity} = \frac{\mathrm{Q_{forward}}}{\mathrm{Q_{reverse}}} = \frac{\mathrm{R_{fluid,reverse}}}{\mathrm{R_{fluid,forward}}} = \frac{\mathrm{L_R W_F}}{\mathrm{L_F W_R}} = \left(\frac{\mathrm{W_F}}{\mathrm{W_R}}\right)^2 \tag{7}$$

2.2 Fabrication process

2.2.1 Photolithography

Standard photolithography technique was used to fabricate the negative molds used to replicate the flow layer and control layer of the check valve and micropump. Briefly, SU-8-3025 (MicroChem, Newton, MA, USA), a thick negative photoresist, was spincoated onto a 100 mm silicon wafer. The wafer was softbaked on a hotplate at 90 °C for 13.5 minutes. A transparency photomask (CAD/Art Services, Inc., Bandon, OR, USA) was placed in contact to the softbaked photoresist and exposed to UV using a Canon Mask Aligner PLA-501F (Canon Inc, Tokyo, Japan). Following exposure, the wafer was postbaked on a hotplate in two stages at 65 °C for 1 minute and 90 °C for 4 minutes. The wafer was placed in SU-8-Developer (MicroChem, Newton, MA, USA) for 13 minutes to remove any uncrosslinked

photoresist. Finally, the wafer was hardbaked for 20 minutes in a 150 °C oven to further crosslink photoresist hardening the mold.

2.2.2 Soft lithography

Inverse images of the SU-8 molds were replicated using Sylgard 184 (Dow Corning, Midland, MI, USA), commonly known as polydimethylsiloxane (PDMS), and standard soft lithography [37] as shown in Figure 2.3.

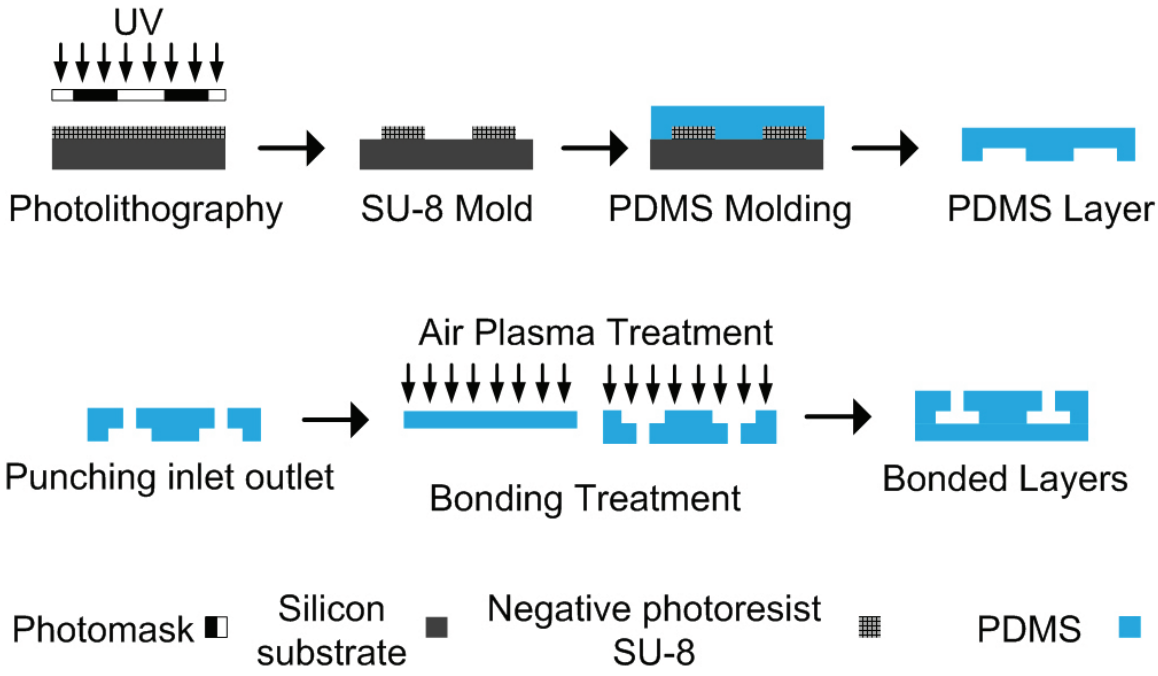

Figure 2.3 Soft lithography technique used in fabricating check valve and micropump.

PDMS, a compliant polymer, has long been the material of choice in fabricating microfluidic devices due to its ease in prototyping and biocompatibility [38, 39]. The PDMS was mixed at a curing agent to base ratio of 1:10 in an ARE-250 mixer (THINKY USA, Laguna Hills, CA, USA) for 2.5 minutes and degassed for 1.5 minutes. Next, the liquid PDMS was poured over

the SU-8 mold, degassed in a vacuum desiccator and cured in a 65 °C oven for a minimum of 6 hours.

After peeling the PDMS replica from the SU-8 mold, the inlet and outlet connections to the valve channel were punched using Ø0.5 mm Harris Uni-Core coring needle (Ted Pella Inc, Redding, CA, USA). In order to inject microspheres into the valve chamber, a third hole was punched in the channel which intersects the valve chamber directly, called the microsphere inlet channel. The check valve layer along with a separate layer of flat PDMS was placed in air plasma (Harrick Plasma, Ithaca, NY, USA) for 60 seconds for surface activation. The PDMS layers were bonded by placing activated surfaces together and applying slight pressure. The PDMS check valve was then placed in a 65 °C oven for 2 hours to strengthen the bond.

Figure 2.4 and Figure 2.5 shows the PDMS layers which form the micropump used in characterization studies and in the trial drug study, respectively.

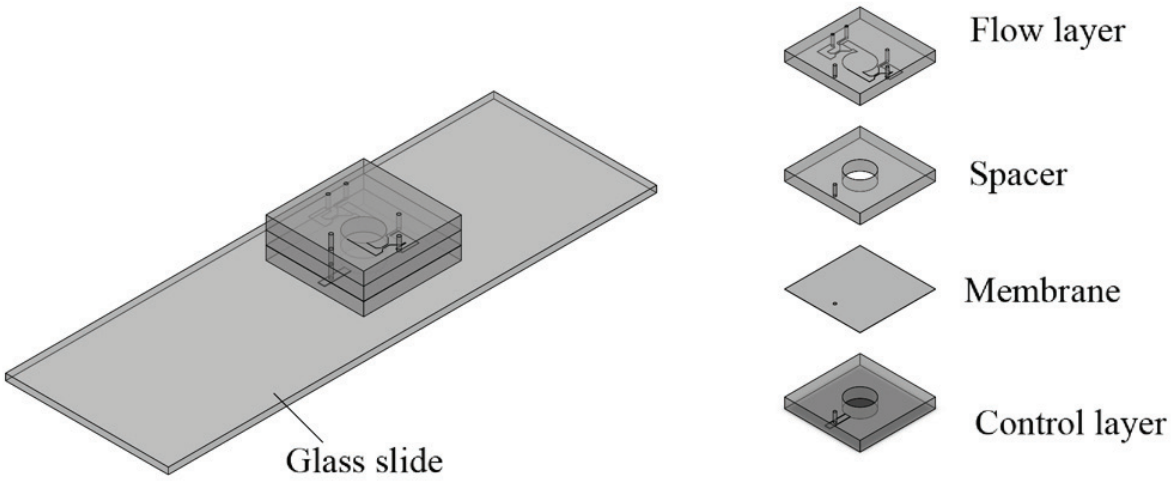

Figure 2.4 PDMS layers used to fabricate micropump in characterization experiments.

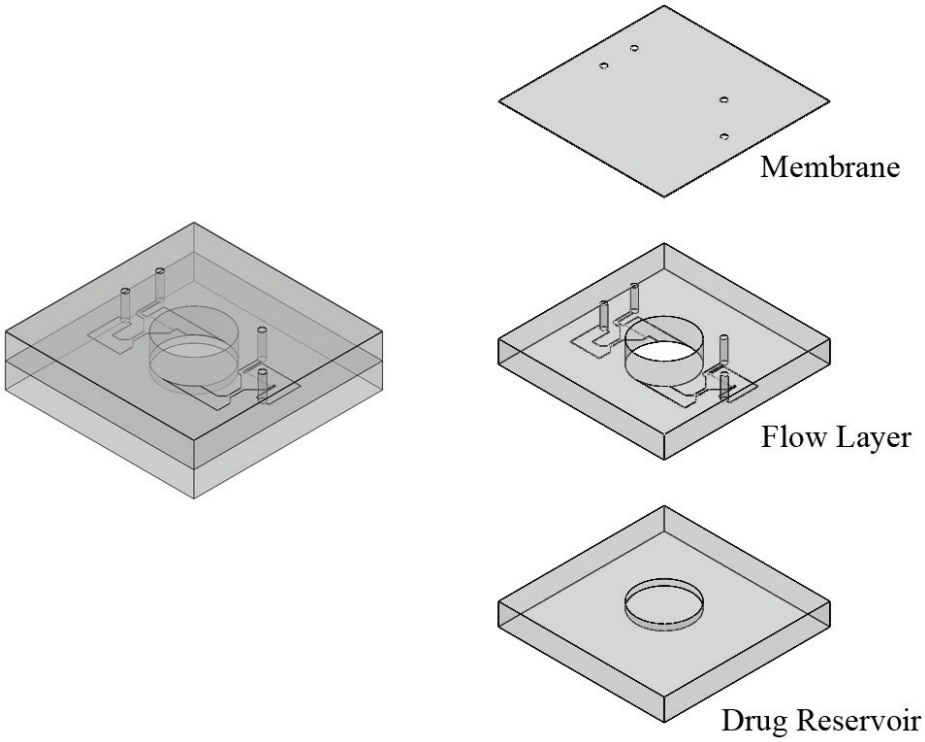

Figure 2.5 PDMS layers of manually actuated micropump used in trial drug diffusion study.

The control layer and flow layer were fabricated using soft lithography. The control layer facilitates pressure application to deflect the diaphragm. The inlet and outlet holes to the pump along with inlets for microsphere injections were punched in the flow layer using Ø0.5 mm coring needle. Another Ø0.5 mm hole is punched at the centre of the pump chamber to allow for easy fluid filling and flushing of the device. The spacer layer was fabricated by cutting a ~1.5 × 1 cm^2 × 0.3 cm thick piece of PDMS, casted in a flat Polyurethane mold, and punching a Ø5 mm through hole. This spacer layer prevents the PDMS diaphragm from bonding to other surfaces during the bonding process, and provides ample stroke volume. PDMS was spun onto the treated silicon wafer at 1400 RPM for 60 seconds using a WS-400-

6NPP-LITE spin coater (Laurell Technologies, North Wales, PA, USA) to fabricate a PDMS diaphragm with a thickness of ~40 μm. Since PDMS has a tendency to stick to silicon wafers due to a thin oxide layer which forms on the surface of silicon wafers, the wafer was silanized using hexamethyldisiloxane (HMDS).

The bonding steps to fabricate the micropump for volume flow studies were as follows:

1. Bonded flow layer to spacer layer
2. Bonded bottom side of spacer layer to diaphragm layer on treated silicon wafer
3. Peeled device with diaphragm attached from silicon wafer, bond bottom side of diaphragm layer to control layer. After bonding all PDMS layers of the micropump was complete a through hole was punched using a Ø0.5 mm Harrris Uni-Core in the inlet channel of the control layer
4. Bonded control layer to glass slide

Steps 1 and 3 required careful edge alignment of the 5 mm punched through holes. This ensured that volume changes in the control layer would result in similar volume changes in the pump chamber.

2.3 Experimental method

2.3.1 Check valve and micropump characterization setup

The MAESFLOW system, which integrates the Microfluidic control system (MFCS) external pressure control system along with the FLOWELL flow sensor (Fluigent, Paris, France), was

used to measure the performance of the check valve and micropump. The 8-port 1000 mbar (100 kPa) MFCS was used in all characterization tests. When calibrated, the MFCS has a output pressure precision of <2.5% of the full scale (corresponding to <250 Pa), and a minimum output pressure step of 95 Pa. The uncalibrated FLOWELL flow sensor can measure a minimum and maximum flow rate of 0.25 μL min^{-1} and 7 μL min^{-1} respectively. When calibrated, the flow sensor can measure flow rates down to 0.1 μL min^{-1}. The resolution and repeatability of the flow sensor at the minimum flow rate is 1.8 nL min^{-1} and 0.8% of the measured value.

An image of the experimental setup is shown in Figure 2.6. 100 μm ID polyetheretherketone (PEEK) tubing connected the pressurized fluid reservoirs to the FLOWELL to minimize flow fluctuations due to tubing compliance. The PEEK tubing exiting from the FLOWELL was attached to 0.5 mm ID flexible tubing (Cole-Parmer, Illinois, USA) and fitted with a 23 gauge stainless steel tip (New England Small Tube, Litchfield, NH, USA) to facilitate connection to the microfluidic device.

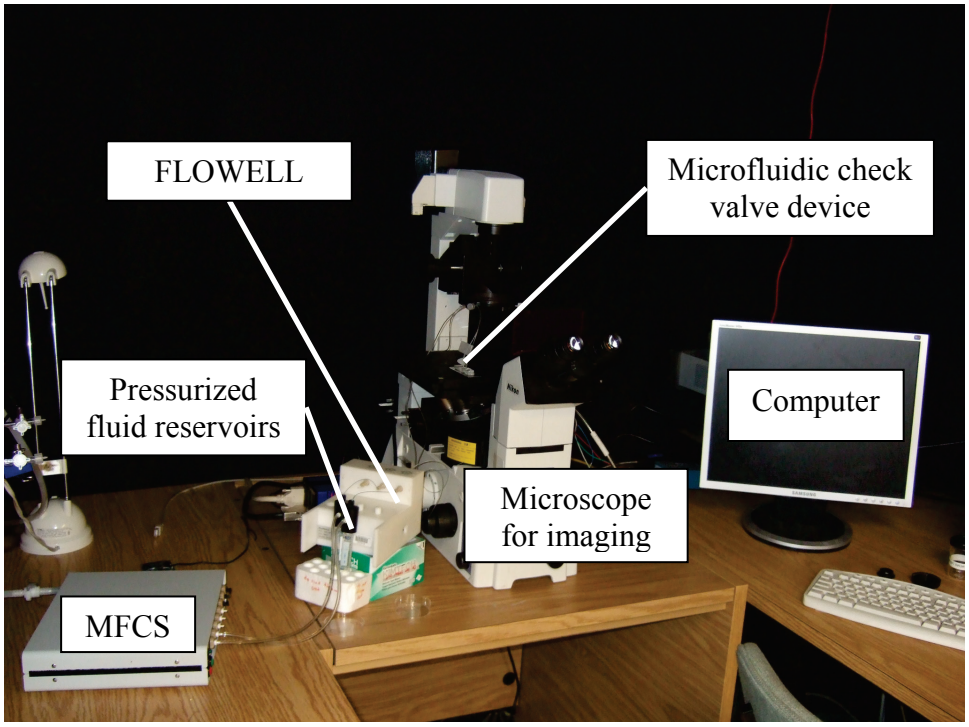

Figure 2.6 Image of the of experimental setup

The microfluidic device was flushed with 5% v/v Tween-20 (Sigma-Aldrich, Canada) aqueous solution before loading the Ø20 µm PS microspheres (Polysciences Inc, Warrington, PA, USA). Tween-20 solution was also used as the fluid medium during characterization to prevent PS microspheres from adsorbing onto PDMS surface. Ø20 µm PS microspheres in DI water were placed in a pressurized fluid reservoir and injected to the valve chamber of the device through the microsphere inlet channel. After an adequate amount of microspheres were introduced, the microsphere inlet channel was blocked off using a blocked 23 gauge stainless steel tip.

For check valve characterization, a fluidic circuit was created by connecting fluid tubing to the inlet and outlet of the check valve device. A schematic of the check valve characterization setup is shown in Figure 2.7.

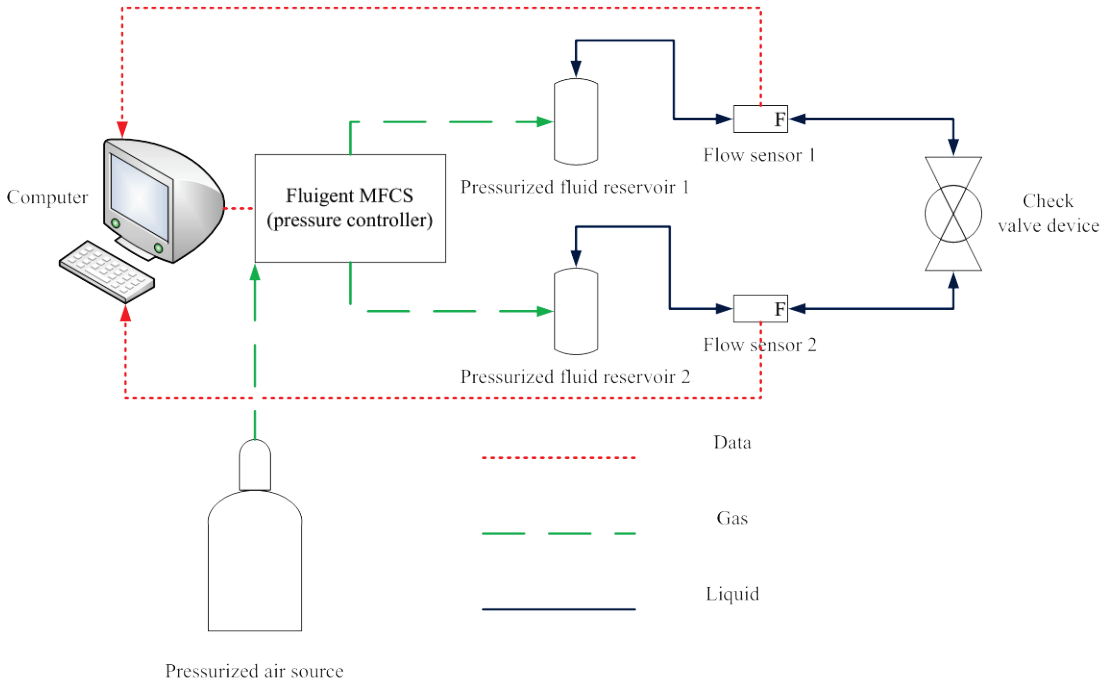

Figure 2.7 Schematic of the check valve characterization setup

A computer controlled the MFCS which generated precise air pressures to the fluid reservoirs. The pressurized air in the pressurized fluid reservoir caused fluid to flow from the fluid reservoirs through the flow sensors and into the check valve device. Flow measurements were made to and from the two fluid reservoirs which correspond to fluid flow through the check valve device. Figure 2.8 shows the check valve device with the stainless steel tips inserted at the inlets on the left and right. In between the inlet and outlet connections is the blocked stainless steel tip which was used to seal off the microsphere inlet channel. A detailed description of check valve characterization procedure can be found in Appendix B.1.

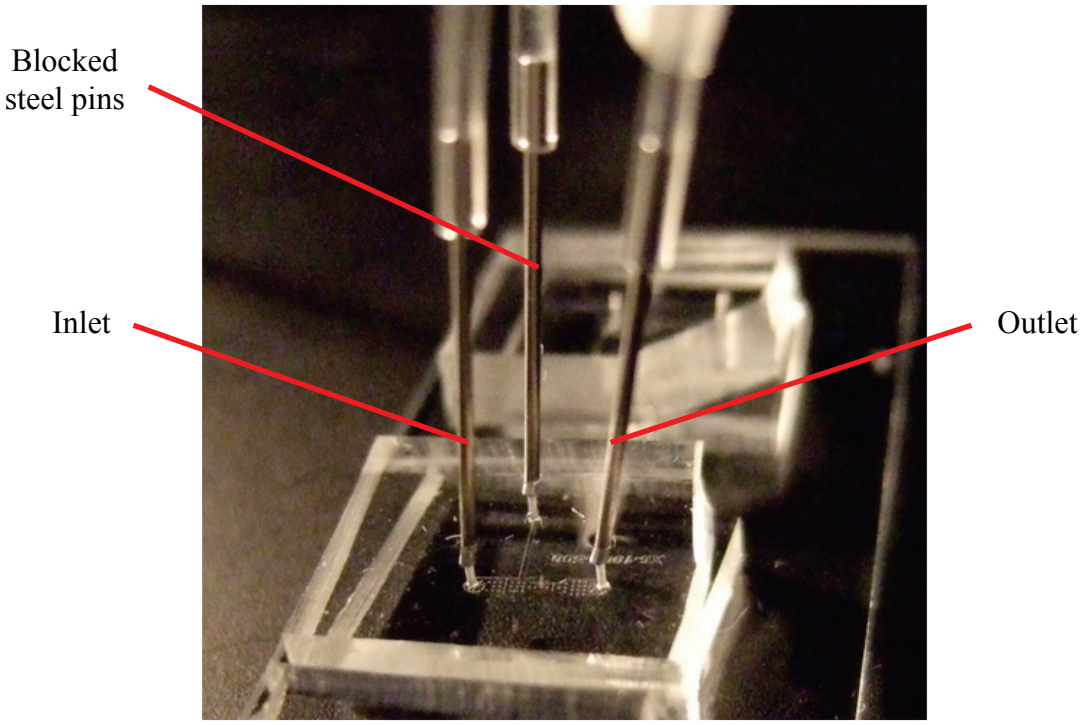

Figure 2.8 Image of check valve device with fluid connection pins on the left and right. A blocked steel pin is shown in the middle to close off the microsphere inlet channel after microspheres are injected.

The applied pressures and durations were controlled using a MAESFLOW script and the direction of pressure bias determined the direction of flow in the channel. A recording script, which ran simultaneously with the pressure control script, recorded the pressure values along with the flow rates of the two reservoirs at 0.1 second intervals. Each pressure step was applied for a duration of 10 seconds. The flow rate values were calculated by taking the average of the last 50 measured data points (corresponding to the last 5 seconds of the pressure step). Figure 2.9 shows the flow rate response to pressure step increases in a 250-2000 μm check valve with approximately 575 microspheres in the check valve chamber. It can be seen that the system reached steady state within the first 5 seconds of the applied

pressure difference, thus flow rate measurements in the last 5 seconds at each pressure step represented the steady state flow rate. The maximum steady state error was 8.5% at an applied difference pressure of 200 Pa.

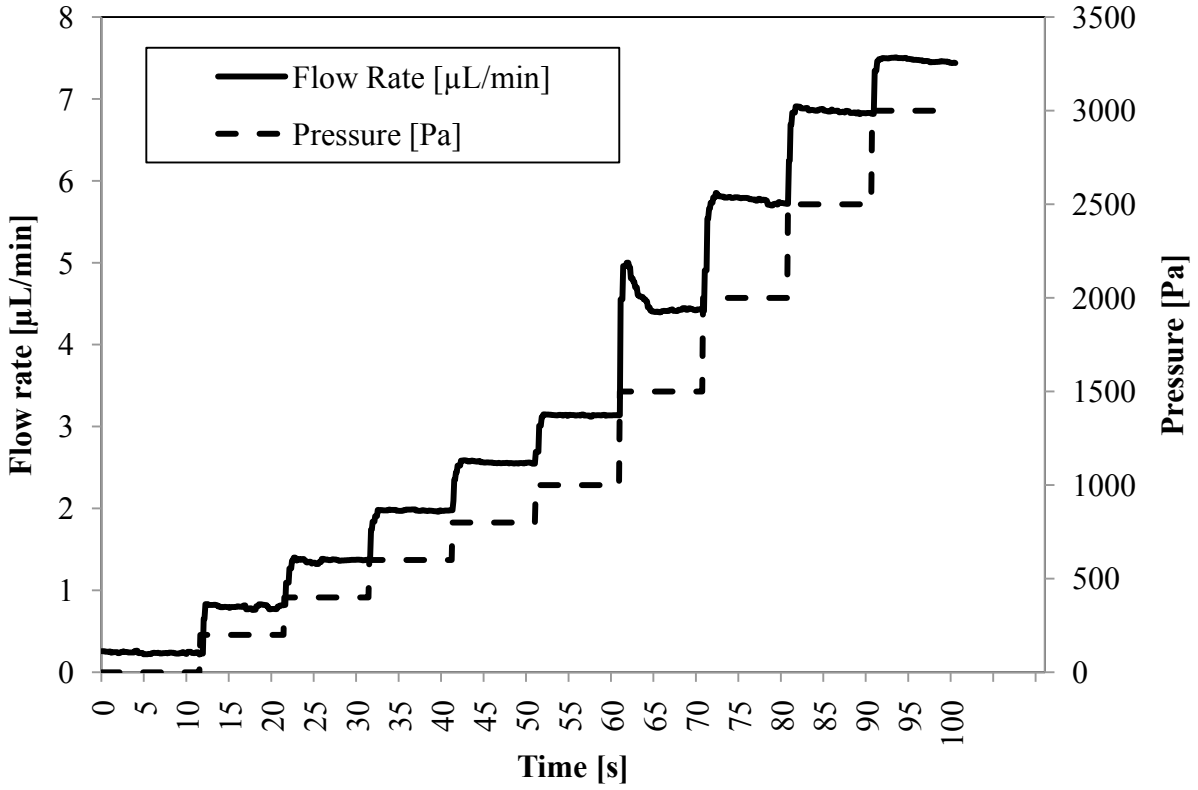

Figure 2.9 Flow rate response time with increasing pressure steps

Figure 2.10 shows the schematic of the system used in testing the micropump. A computer was used to control the output pressure from the MFCS. The computer also programmed the USB 6212 data acquisition module using Labview VI (National Instruments, USA) to control the cycle time and duty cycle of the solenoid valve. The solenoid valve provided on-off control of the pressure in a fluid reservoir which was connected to the control layer of the micropump. When the solenoid valve opened, pressurized air caused fluid to flow from the pressurized fluid reservoir into the control layer. The fluid flow in the control layer deflected

the PDMS diaphragm resulting in the pump chamber compression. When the solenoid valve closed, the pressure in the pressurized fluid reservoir was vented to atmosphere, and the PDMS diaphragm deflected back to its equilibrium state resulting in the pump chamber decompression. As shown in Figure 2.11, steel pins were connected to the inlet and outlet of the micropump with blocked steel pins closing off the microsphere inlet channels and extra inlet to the pump chamber which facilitated filling and flushing of the device. Flow from the micropump was measured using the FLOWELL system. A detailed description of check valve characterization procedure can be found in Appendix B.2.

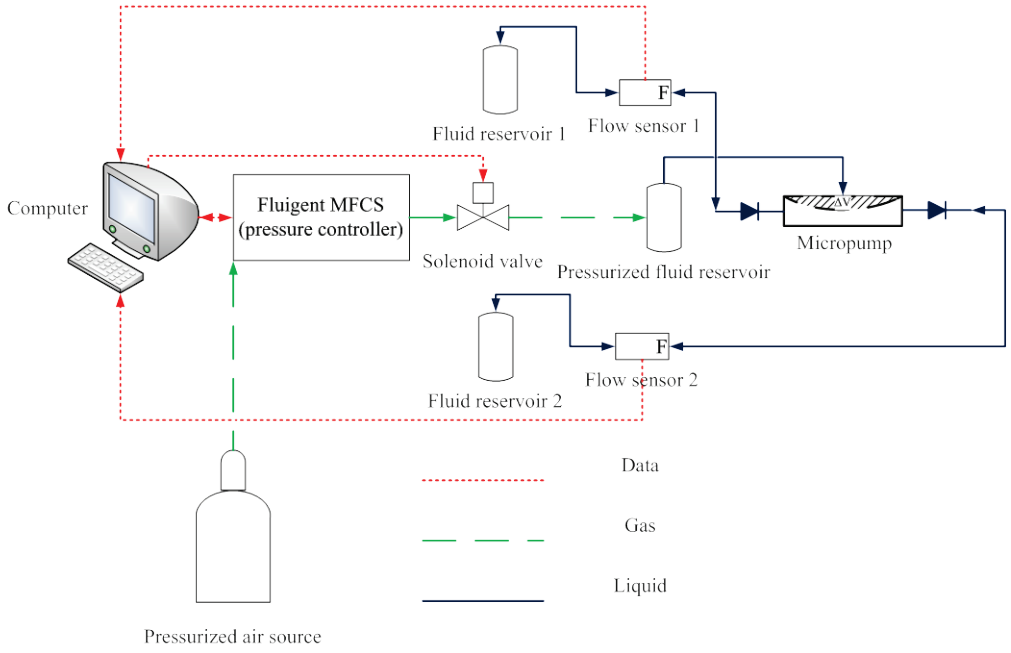

Figure 2.10 Schematic of the micropump characterization setup

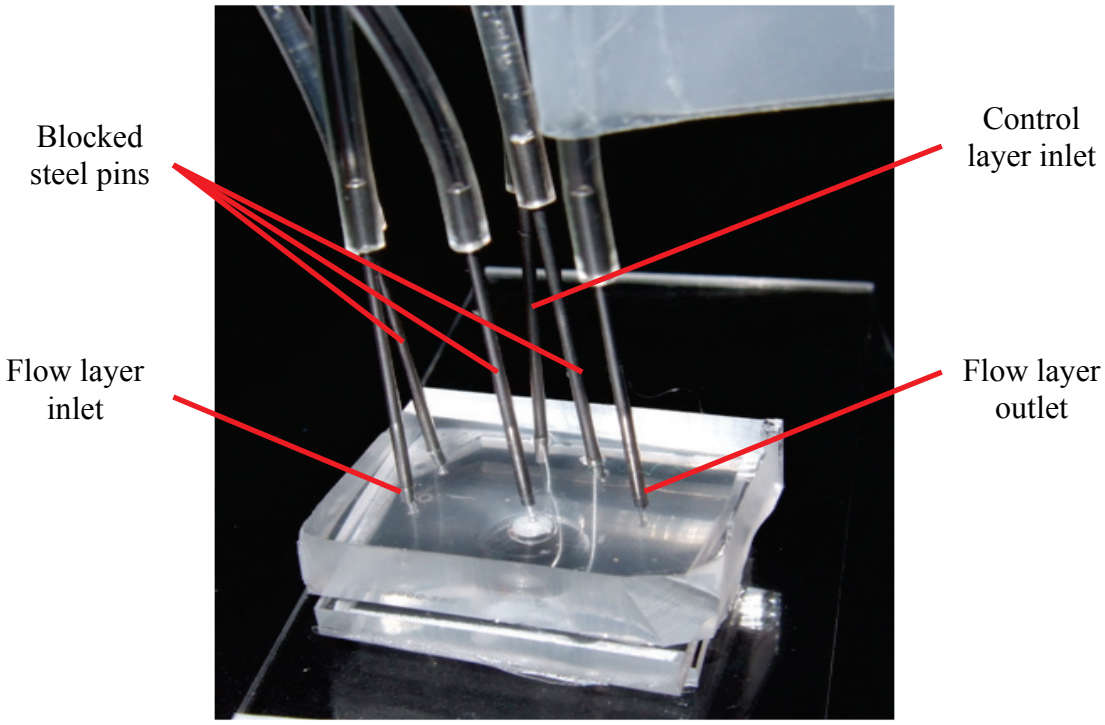

Figure 2.11 Image of micropump with fluid connection pins. Blocked steel pins are shown to close off the microsphere inlet channels after microspheres are injected in the check valves at the inlet and outlet side of the pump chamber. A blocked stainless steel pin closes off an inlet channel to pump chamber. The inlet to the pump chamber was created to allow for easy filling and flushing of the micropump.

2.3.2 Trial drug study

A drug reservoir with concentrated drug, as shown in Figure 2.5, was fabricated to produce the drug delivery micropump. The drug delivery system had a Ø5 mm × ~550 µm deep drug reservoir. To load the drug reservoir, a 20 mg mL^{-1} mixture was created by dissolving tritium labeled DTX and unlabeled DTX in a 50/50 ethanol and dichloromethane (DCM) solution. 100 µg of drug was deposited into the PDMS reservoir by depositing 10 µL of the DTX

solution and allowing the solution to evaporate. The solution was deposited in 5 μL intervals to prevent the reservoir from overflowing.

Two micropumps were used in the trial drug study, one micropump with no microspheres in the valve chamber and another micropump with ~1000 microspheres in the inlet and outlet valve chambers were placed in separate vials with 4 mL of sterile 1% w/v bovine serum albumin (BSA) + phosphate buffered saline (PBS) solution. Both micropumps were initially primed three times using manual actuation. The micropump with no microspheres was manually primed by blocking the inlet then outlet of the micropump during diaphragm deflection and relaxation respectively. Each actuation consisted of applying the manual load for 2 minutes and waiting 6 minutes to ensure the diaphragm had sufficient time to deflect and DTX could reach its solubility limit in the drug reservoir. The amount of drug released into 1% BSA+PBS solution was measured to ensure the device was operational and the micropump's channels were filled with drug solution before commencing the drug diffusion experiment.

DTX released from each micropump in 1% BSA+PBS solution was measured by removing the entire solution in the vial and performing the drug extraction procedure. First, 300 μL of DCM, an organic solvent, was added to the solution and vortex mixed for 60 seconds to dissolve and extract DTX into DCM. DTX along with protein molecules in the 1% BSA+PBS solution precipitated with the organic solvent. The solution was left for 10 minutes to separate the liquid phase from the organic phase which contained DTX. Subsequently, the liquid phase was aspirated out and the remaining organic phase was vortex mixed with 5 mL of CytoScint liquid scintillation fluid (Fisher Scientific, Fair Lawn, NJ, USA) for 5 seconds. After the liquid was transferred into scintillation vials, the vial was

placed in a LS 6500 series multi-purpose scintillation counter (Beckman Coulter Inc, Brea, CA, USA) to measure the disintegrations per minute (DPM). The DPM reading is a measure of DTX in the liquid solution. A standard curve, which relates the amount of DTX to its corresponding DPM reading, was created by introducing varying volumes of stock drug solution at 20 mg mL^{-1} into 1 mL of 1% BSA+PBS solution and following similar drug extraction steps.

Before each diffusion experiment both micropumps were manually primed in 4 mL of 1% BSA+PBS solution to ensure fully saturated DTX solution filled the micropump chambers. Afterwards, the solution in the vial was removed and replaced with 4 mL of sterile 1% BSA+PBS. The vial was then placed in the fridge to study DTX diffusion from the device over 24 hours.

To measure the amount of drug released in one actuation, the micropump with microspheres in the valve chamber was placed in a vial with 4 mL of sterile 1% BSA+PBS and actuated manually with a weighted plastic cylinder. The plastic cylinder had a Ø3 mm and weighed 1.26 g cylinder translating to a pressure of ~ 1.75 kPa. The one time actuation experiment was repeated three times.

Chapter 3: **Check valve results and discussion**

3.1 Porous media length

The number of microspheres and porous media length was measured using image analysis software ImageJ. The number of microspheres was rounded to the nearest 25 with the porous media length rounded to the 10 μm. Table 3.1 presents the number of microspheres used in testing the check valves.

Table 3.1 Approximate number of microspheres in valve chamber corresponding to porous media lengths L1, L2, and L3

	Microspheres[a]			Porous media length in narrow channel[b] [μm]		
Check Valve	L1	L2	L3	L1	L2	L3
250-500 μm	125	425	675	200	670	1100
500-1000 μm	275	575	850	230	460	690
250-2000 μm	225	275	575	340	450	920

[a]Rounded to the nearest 25, [b]Rounded to nearest 10 μm

The ability to make a quality seal at the microsphere inlet channel was important in controlling the number of microspheres injected into the valve chamber. Figure 3.1 shows microspheres forming porous media at PDMS pillars in the reverse and forward flow directions. A poor seal would result in microspheres flowing from the valve chamber back into the microsphere inlet channel. When a blocked steel pin was inserted to close off the microsphere inlet channel, there was a chance of trapping small air bubbles which created voids in the channel. Upon removing the air bubbles trapped in the microfluidic device by pressurizing the fluid channel, some microspheres from the valve chamber escaped back into the microsphere inlet channel. Furthermore, if the void produced by the air bubble was not

removed from the device before characterization, it introduced compliance in the valve which caused some microspheres to partially flow into the microsphere inlet channel at higher pressures differences. However, microspheres would temporarily travel into the microsphere inlet channel and flow back in the check valve chamber during experimental testing. During check valve characterization a maximum of 10 microspheres would flow from the valve chamber and be trapped in the microsphere inlet channel. In the worst case scenario, with the least amount of microspheres in the valve chamber, 10 microspheres trapped in the microsphere inlet channel represented <8% of the total amount of spheres in the check valve, thus it had negligible effect on the porous media length and check valve characterization.

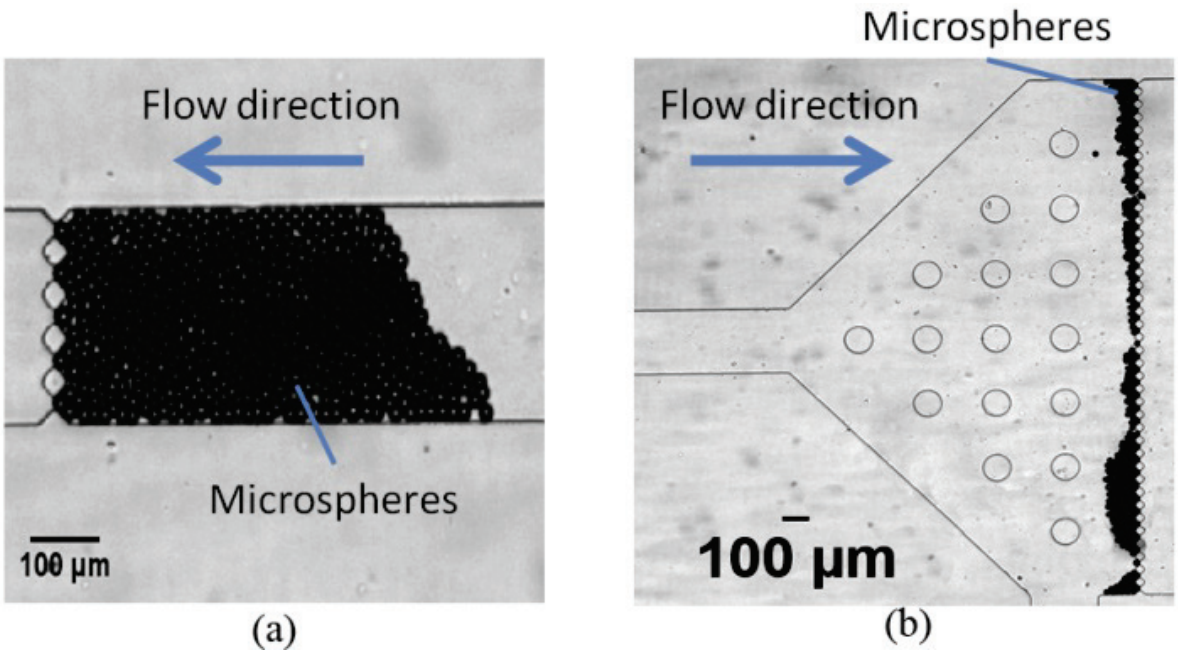

Figure 3.1 (a) Microspheres collecting in reverse flow direction, (b) microspheres collecting in forward flow direction.

3.2 Check valve performance

The three check valve designs (250-500 μm, 500-1000 μm and 250-2000 μm) with different number of microspheres (L1, L2 and L3 as listed in Table 3.1) were experimentally tested. A pressure difference between 200 Pa and 3000 Pa was applied between the inlet and outlet of the check valve device generating flow. Flow measurements for each test case were performed three times and the porous media were reformed before each test to create variations in the porous media formed before each measurement. To reform the porous media the microspheres were flowed in the opposite direction of testing for 0.5 seconds under a pressure difference of 100 Pa before flowing in the direction of testing under a pressure difference 100 Pa. Once the microspheres collect on the PDMS pillars, small flow oscillations in the forward and reverse directions were created by manually striking the stainless steel inlet and outlet connection pins. The small flow fluctuations helped form porous media which packed even across the width of the channel. Flow rate measurements for each porous media length were performed in one direction of flow (starting in the reverse direction) then subsequently reversed to measure flow in the opposite direction.

Figure 3.2 shows the performance of the 250-2000 μm check valve with no microspheres in the valve chamber. The flow rate figures for the 250-500 μm and 500-1000 μm check valves can be found in the Appendix C. As expected, the flow rate increased linearly with applied pressure difference as described in Eq (1). The flow rates in the reverse and forward directions for each applied pressure difference are equal, as depicted by the overlapping data points. Thus, the fluid resistance in the reverse and forward flow directions of the check valve with no microspheres is the same. Consequently, by introducing microspheres into the

valve chamber, any channel resistance change due to the flow direction is attributed to the microspheres' effects.

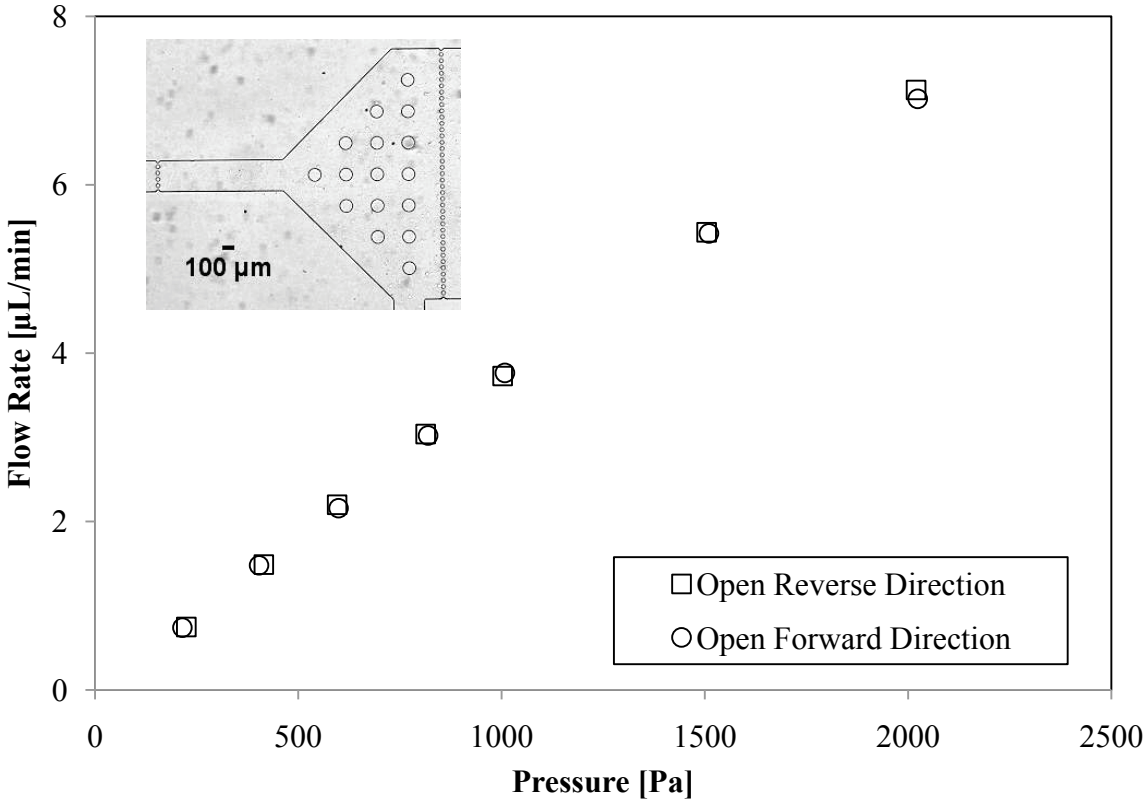

Figure 3.2 Flow rate of valve channel with no microspheres for 250-2000 µm check valve.

Figure 3.3 shows the flow rates versus applied pressure difference based on the porous media length and flow direction for the 250-2000 µm check valve. The flow rates represent the average of three measurements, and the error bars representing one standard deviation from the mean were too small to show clearly in the figure. The flow rate increased linearly with applied pressure difference similar to that of the check valve with no microspheres in the valve chamber. However, the flow rates in the reverse and forward directions differed due to the difference in channel resistance provided by the porous media.

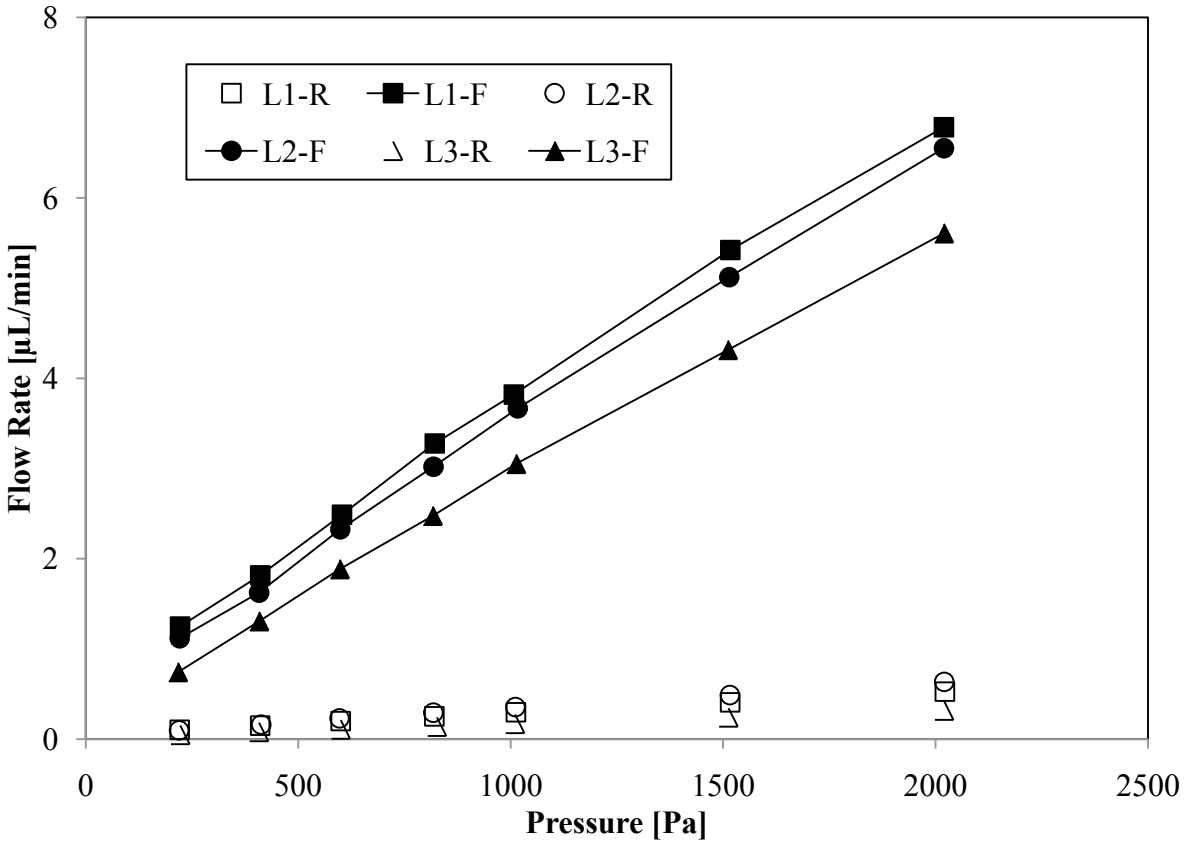

Figure 3.3 Flow rate versus pressure difference at porous lengths L1-L3 (see Table 3.1) for 250-2000 µm check valve.

The diodicity of the 250-2000 µm check valve with porous media lengths L1-L3 is calculated and shown in Figure 3.4. Each data point represents the average diodicity calculated from the three flow rates in the reverse and forward directions. The error bars represent one standard deviation from the mean (n=3). With open channels (no microspheres in the valve chamber), the fluid resistance in the check valve between the retaining PDMS pillars can be calculated by summing the resistance in each section of the channel calculated using Eq (8).

$$R_{\text{fluid ,section}} = \frac{12\mu L}{WH^3}\left[1 - \frac{H}{W}\left(\frac{192}{\pi^5}\sum_{n=1,3,5\ldots}^{\infty}\frac{1}{n^5}\tanh\left(\frac{n\pi W}{2H}\right)\right)\right]^{-1} \quad (8)$$

The 250-2000 μm check valve with channel height of 35 μm has a theoretical fluid resistance of 1.5×10^{12} Pa s m^{-3}. In low Reynolds Number flow viscous forces dominate such that the fluid resistance in the check valve with open channels is equal in the reverse and forward flow direction. Therefore, a check valve with no microspheres in the valve chamber has a theoretical diodicity of 1. It can be seen in Figure 3.4 the measured diodicity of the check valve with no microspheres in the valve chamber shows good agreement with the theoretical diodicity.

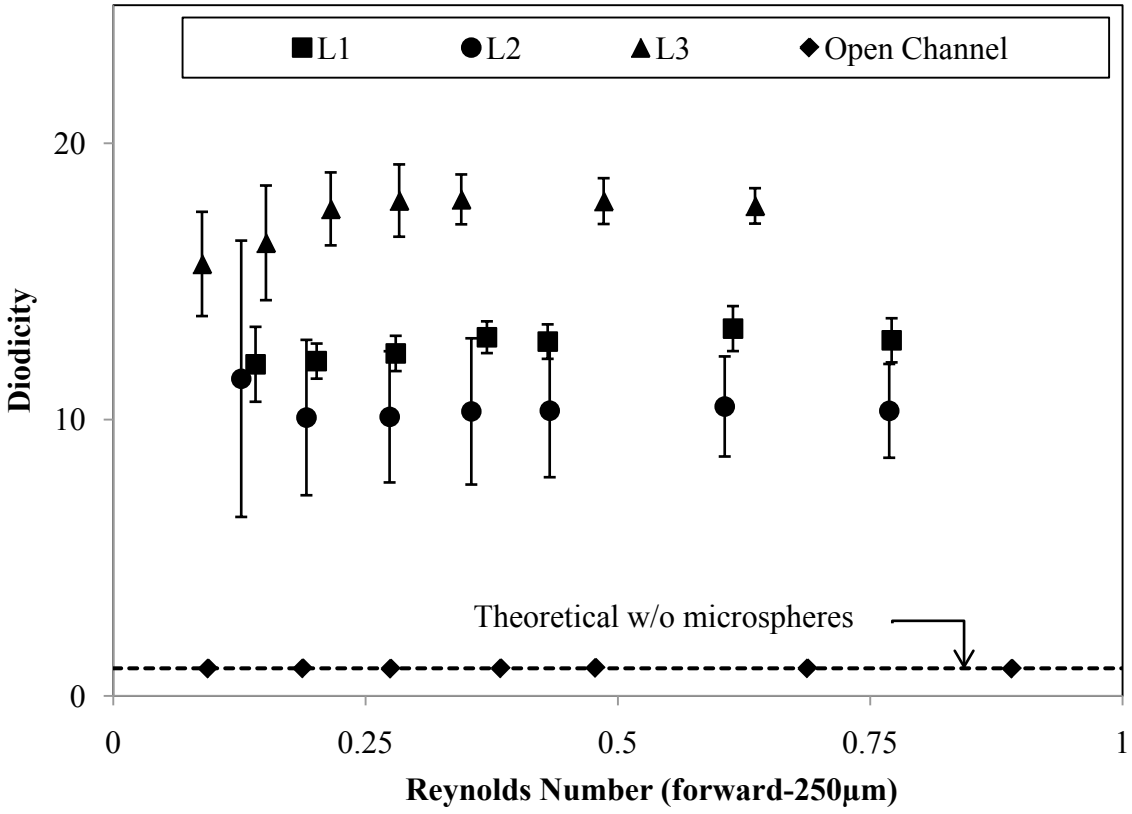

Figure 3.4 Diodicity of valve based on porous lengths for 250-2000 μm check valve. Error bars represent one standard deviation from the mean (n=3).

With microspheres injected into the valve chamber forming porous media lengths L1-L3, the 250-2000 μm check valve was tested under low flow rates generated by pressures between 200 Pa and 3000 Pa. The 250-2000 μm check valve had a minimum diodicity of 10.1 and a maximum diodicity of 18.0. However, a diodicity of 64 was calculated for the 250-2000 μm microsphere check valve using Eq (5). Although the 250-2000 μm check valve had a lower measured diodicity than expected, the 250-500 μm and 500-1000 μm check valve with L3 long porous media lengths performed close to its theoretical diodicity. The results showed the check valve performing well under low pressures and low flow rates. In contrast to the 250-2000 μm check valve's minimum diodicity of 10.1, diffuser valves require high Reynolds Number flow and only exhibit a diodicity of 1.5 [30]. Furthermore, Loverich et al's PDMS cantilever flap check valve produces a diodicity of 1.5 at Re=1 [26]. Similarly, Yang and Lin's PDMS cantilever flap check valve performed poorly under low pressures and had a diodicity of about 1, which meant it did not rectify flow at low pressures [27]. Therefore, the microsphere check valve represents a significant performance improvement over the other thin planar check valves such as diffuser and cantilever type check valves reported.

We hypothesize the reason for the lower than expected value is the porous media formed in the reverse direction has significant leakage especially with a low number of microspheres. A low number of microspheres can lead to poor packing and inconsistent porosity in the porous media leading to significant fluid leakage. The longest porous media length (L3) formed in the 250-2000 μm check valve chamber with 575 microspheres. We hypothesize that increasing the number of microspheres in the valve chamber would bring the check valve diodicity closer to the theoretically calculated value. Furthermore, it was expected that the experimental diodicity for L2, should be greater than the diodicity of L1. However, the L1

diodicity measurements were within the error of in diodicity measurement for L2. This may be due to L1 and L2 having low number of microspheres in the valve chamber corresponding to short porous media lengths 340 µm and 450 µm respectively which were similar.

The diodicity figures for the 250-500 µm and 500-1000 µm check valve are shown in Figure 3.5 and Figure 3.6. Similar to the 250-2000 µm check valve, the diodicity of the 250-500 µm and 500-1000 µm check valve with no microspheres in the valve chamber is in agreement with the theoretical diodicity of 1.

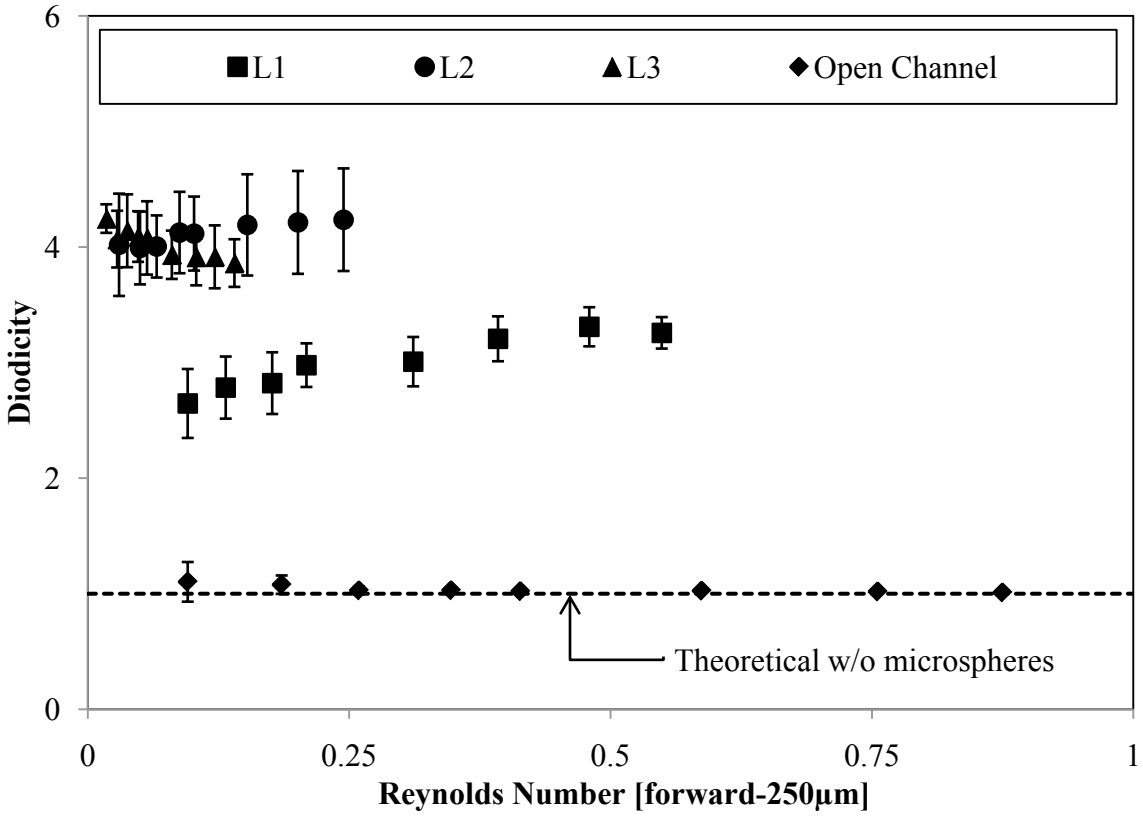

Figure 3.5 Diodicity of valve based on porous lengths for 250-500 µm check valve. Error bars represent one standard deviation from the mean (n=3).

The theoretical diodicity for the 250-500 µm and 500-1000 µm check valve with microspheres in the valve chamber was calculated to be 4 using Eq. (5). For the 250-500 µm check valve the average measured diodicity for L1 with porous media length of 200 µm had a average diodicity of 3.0 which was lower than expected. In contrast, porous media lengths L2 and L3 had average diodicity of 4.1 and 4.0 which matches the theoretically calculated diodicity. The corresponding porous media lengths were 670 µm and 1100 µm respectively. The match between the experimental and theoretical values occurs under low flow rates (Re<0.25). This may be a result of minimized leakage in both directions of flow in the valve due to long porous media lengths formed by a high number of microspheres.

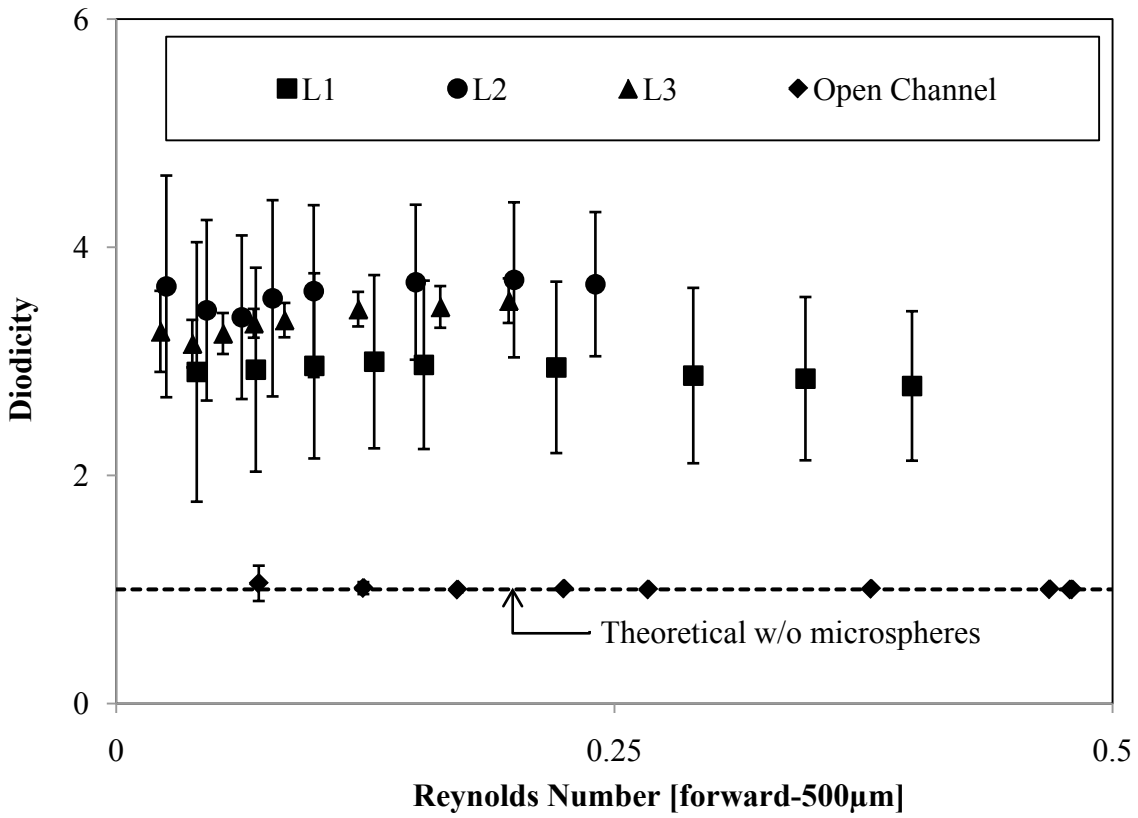

Figure 3.6 Diodicity of valve based on porous lengths for 500-1000 µm check valve. Error bars represent one standard deviation from the mean (n=3).

The measured diodicity of the 500-1000 μm check valve for all three porous lengths were lower than the theoretical diodicity of 4. The average measured diodicity for porous media lengths L1-L3 was 3.3 with large error bars showing variations in the measurement. The large errors in measurement may be due to the wider (500 μm) reverse channel width which caused uneven packing and inconsistent porosity across the channel width. In addition, support pillars were placed in the reverse flow channel where the porous media forms which may have further caused the microspheres to have inconsistent porosity leading to higher leakage.

The measured diodicity figures for the three check valve designs showed a trend of increasing diodicity as the porous media length increased. It was found in pressure filtration studies that cake porosity decreased and leveled off as the cake thickness increased [40, 41]. The cake thickness is equivalent to the porous media length in our check valve. This supports the hypothesis that the check valve will perform closer to its theoretical diodicity with increasing porous media length. The longer porous media length leads to a porous media with a consistent porosity in the reverse and forward direction. With the same level of leakage in both flow directions due to the lower porosity, the check valve should perform up to the theoretical diodicity. Thus, we observed the gradual trend to higher diodicity towards the theoretical diodicity as porous media lengths increased in each check valve design.

Variations and errors in measured diodicity values may be a result of porous media having varying porosities. For example, depending on the direction of flow, the porosity of the porous media may differ. The viscous drag force induced on a single microsphere is given by Stokes law in Eq (9),

$$F_D = 3\pi\mu U d_p \quad (9)$$

where μ is the fluid viscosity, U is the mean flow velocity, and d_p is the diameter of the microsphere. Although Stokes law is based on drag on a single microsphere it is suggested that the drag force on microspheres in the reverse direction is higher than in the forward direction. The drag force on a single microsphere in the reverse direction can be 8 times as high as drag force in the forward direction in the 250-2000 μm check valve. This difference in drag force can cause microspheres to form porous media of varying porosities.

It has been shown in filtration studies that changes in the viscous drag forces acting on particles forms a compressed cake with varying porosity [42]. To demonstrate changes in porosity due to changes in pressure differences, the average porous media length was approximated with the porous media subjected to increasing applied pressures. It can be seen in Figure 3.7 that as the applied pressure increased, the microspheres formed porous media with tighter packing resulting in lower porosity. Using ImageJ the average porous media lengths were approximated and plotted relative to the initial porous length L_0 where there was no applied pressure. The results can is shown in Figure 3.8.

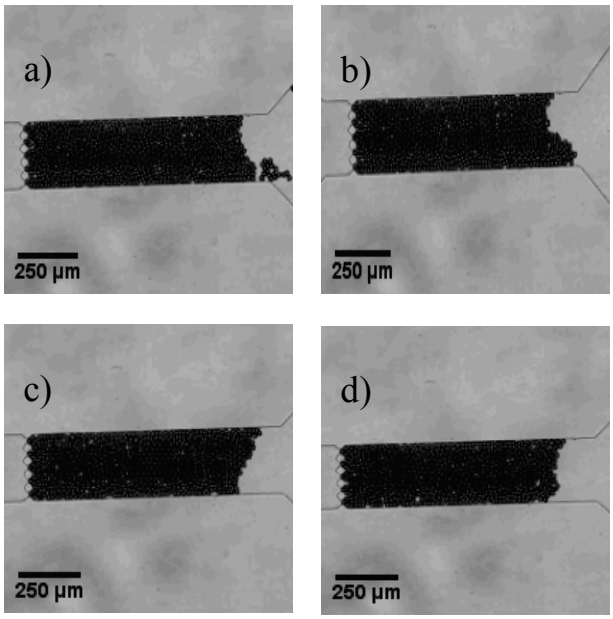

Figure 3.7 Images of microspheres packing in reverse flow direction under applied pressure of: a) 0 Pa, b) 500 Pa, c) 2000 Pa, and d) 3000 Pa

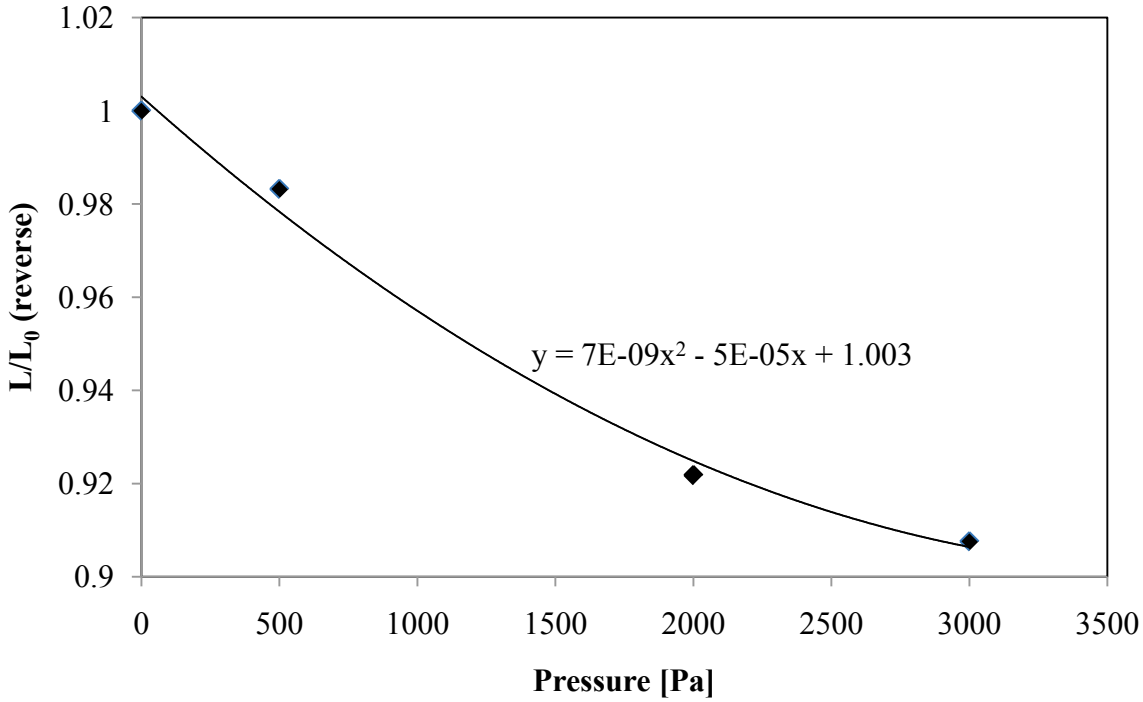

Figure 3.8 Change in porous media length (relative to initial length L_0) due to increasing pressure differences in the reverse flow direction.

To further demonstrate the varying porosities in the check valve Figure 3.9 shows the diodicity of the 250-2000 μm check valve which was characterized in an oscillating flow.

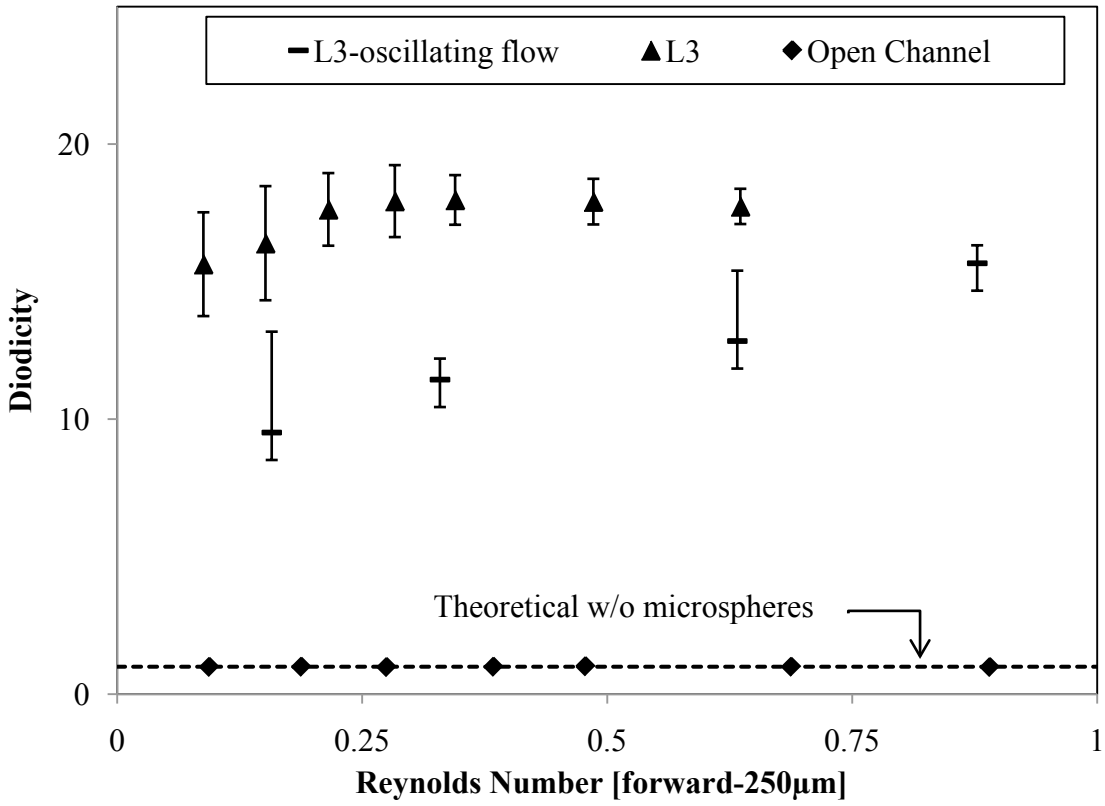

Figure 3.9 Diodicity differences between oscillating flow versus one way flow characterization for 250-2000μm check valve. Error bars represent one standard deviation from the mean (n=3).

In oscillating flow, the flow rate was measured in the reverse direction generated by a pressure bias in the reverse direction. Immediately following the reverse direction flow, the flow rate was measured in the forward direction by switching the pressure bias to the forward direction. This differed from the check valve characterization tests which measured flow rates through porous media in one direction of flow at each pressure step, then repeating in the opposite direction. The results show a trend of increasing diodicity as the flow rate

increased. This may be due to the higher viscous drag force in the reverse flow direction forming porous media with lower porosity.

On the other hand, Figure 3.10 and Figure 3.11 figures show no trend in diodicity when the 250-500 µm and 500-1000 µm check valves were characterized in an oscillating flow. This may be attributed to the lower difference in drag force in the forward and reverse direction causing porous media with inconsistent porosity.

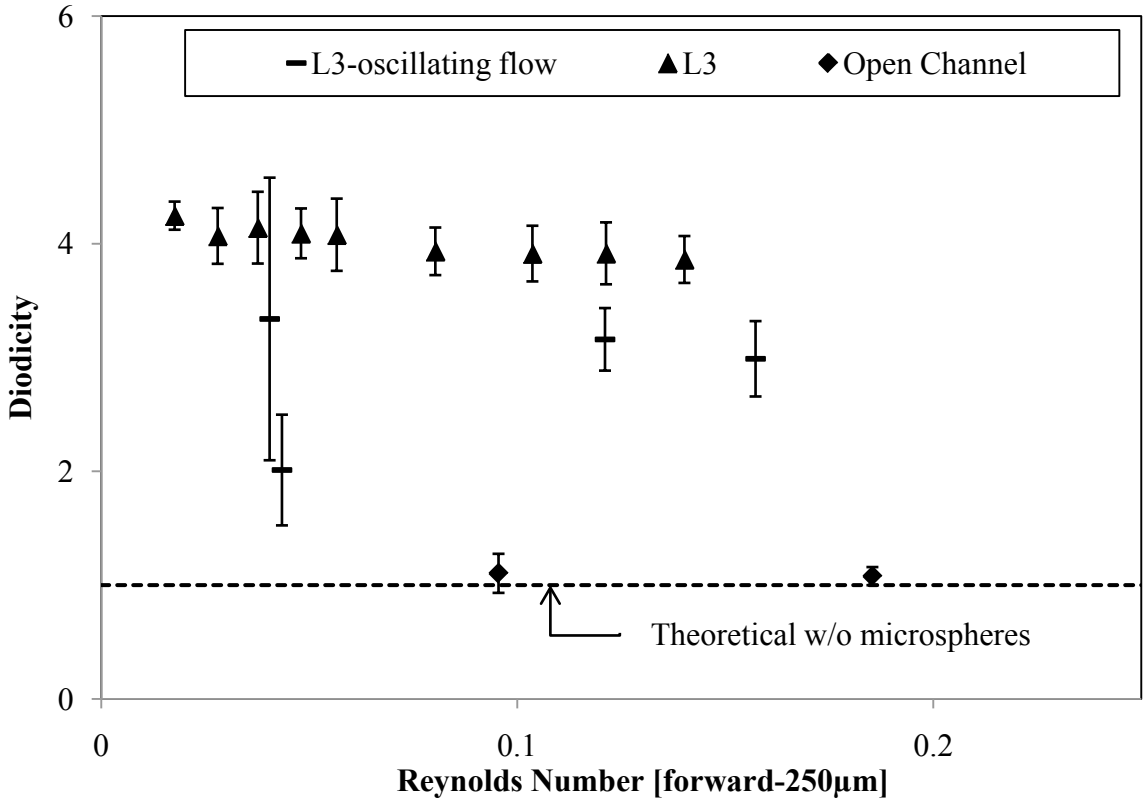

Figure 3.10 Diodicity differences between oscillating flow versus one way flow characterization for 250-500µm check valve. Error bars represent one standard deviation from the mean (n=3).

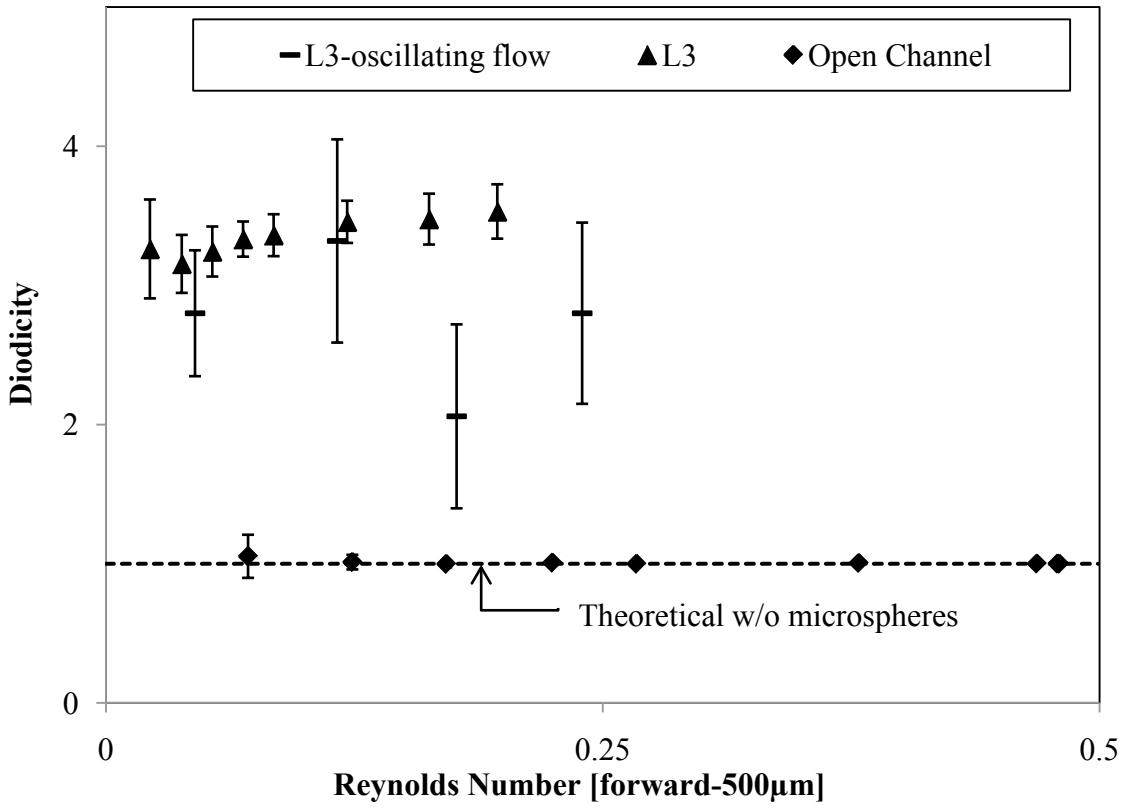

Figure 3.11 Diodicity differences between oscillating flow versus one way flow characterization for 500-1000µm check valve. Error bars represent one standard deviation from the mean (n=3).

Chapter 4: **System performance**

4.1 Pump performance

We investigated the performance of the pumping system using 250-2000 μm check valves in series with a deflecting diaphragm pump chamber. Approximately 900 microspheres were injected into the inlet and outlet valve chambers. Characterization experiments were performed by applying pneumatic pressure between 200-1000 Pa in 200 Pa increments with a duty cycle of 50% and a cycle time of 240 s. An actuation cycle consisted of applying pressure on the diaphragm compressing the pump chamber, and removing the applied pressure decompressing the pump chamber. The duty cycle is defined as the ratio between the duration of applied pressure to the diaphragm and the period of one actuation cycle. The 240 second cycle time was determined experimentally by monitoring the flow volumes at the inlet and outlet after each actuation cycle. However, this cycle time is greatly affected by the hydrodynamic resistance of the FLOWELL and tubing. Cycle times lower than 240 seconds prevented the flexible diaphragm from deflecting to its steady state and also prevented the diaphragm from returning back to its equilibrium state as shown by the increasing gap between the inlet and outlet volume plots. Incomplete deflections to the steady state and equilibrium states can result in inconsistent stroke volumes at each actuation pressure due to the hyperelastic non linear behavior of PDMS [43]. Volume flow plots for 60 seconds and 120 second cycle times can be found in Appendix D.

The micropump was actuated at each applied pressure three times and the volume flow through the inlet and outlet is shown in Figure 4.1.

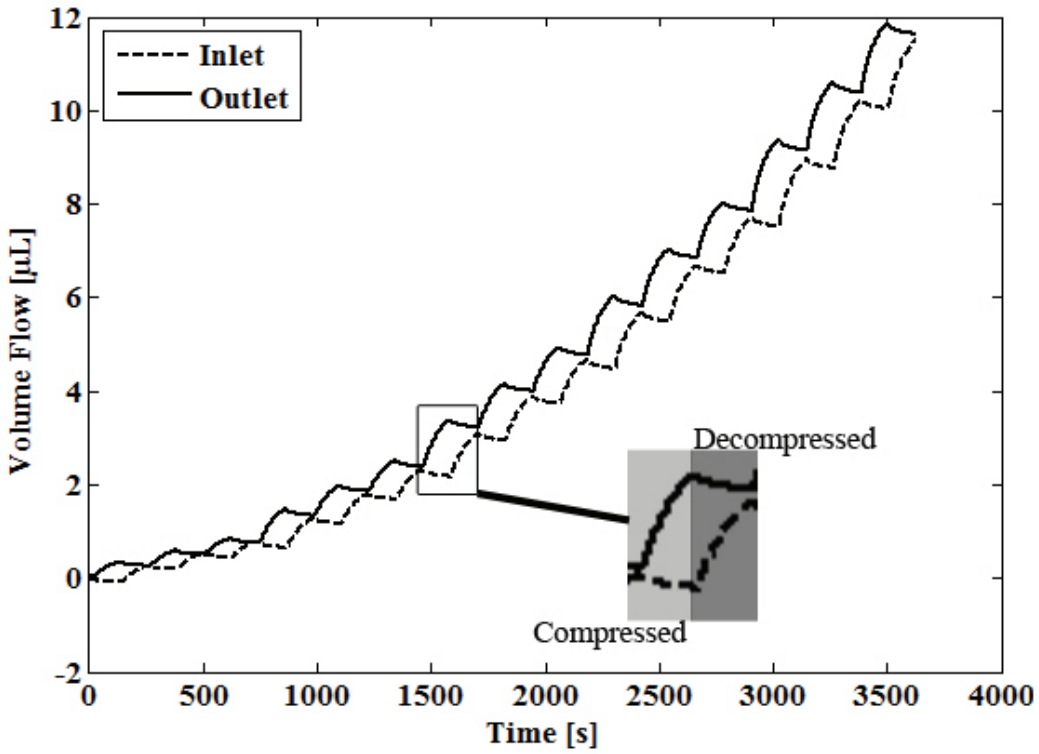

Figure 4.1 Volume flow measurement of micropump with 240 second cycle time and 50% duty cycle. Shaded areas show the volume flow of the micropump at inlet and outlet during one actuation cycle.

It shows that when the pump chamber compressed, it generated flow through the outlet with low reverse flow through the inlet. On the other hand, when the pump chamber is decompressed, a majority of fluid flows through the inlet and fluid is drawn back into the pump chamber from the surrounding environment. As expected, actuating the flexible diaphragm with increasing pressures led to increasing fluid volume displacement. Figure 4.2 shows that that the volume flow from the micropump increased linearly as the actuation pressure increased. The micropump displaced a volume of 0.25 µL with an applied pressure of 200 Pa and displaced a maximum volume of 1.26 µL at 1000 Pa.

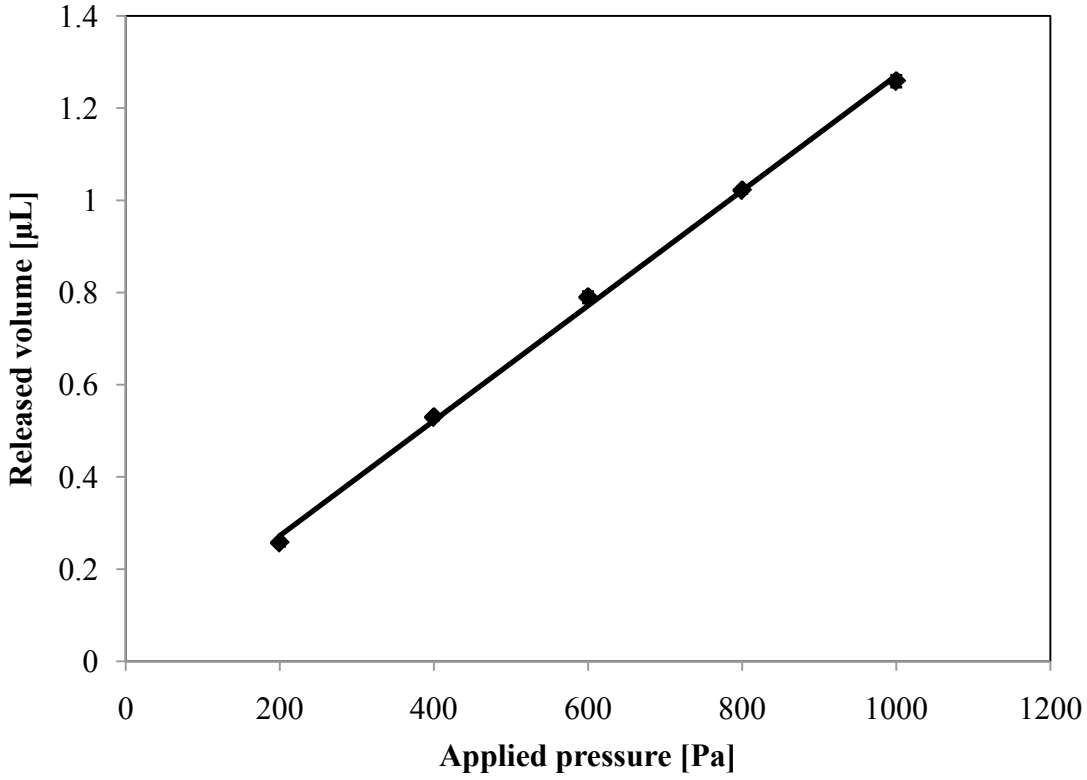

Figure 4.2 The average volume flow versus applied pressure on the diaphragm of a 250-2000 µm check valve micropump. The actuations had a cycle time of 240 seconds with a duty cycle of 50%. Error bars are too small to show clearly and represents one standard deviation from the mean (n=3).

4.2 Trial diffusion drug study

If the micropump is implanted and actuated in the conjunctiva cul-de-sac, fluid tears in the eye is the working fluid which flows into the pump chamber through the inlet check valve and drug solution flows out through the outlet check valve from the pump chamber. The pump chamber is enclosed by the drug reservoir where solid drug will diffuse and reach its solubility limit in the fluid. The two check valves ensure the net fluid flow in one-direction only and also serve to restrict diffusion from the pump chamber when the device is not in

operation. The tortuosity introduced by the porous media formed by microspheres hinders diffusion from the pump chamber [44].

To demonstrate that the check valve has the ability to limit unwanted drug release from the micropump, we studied the diffusion of DTX in a manually actuated drug delivery device as a proof-of-concept. Since this micropump was actuated manually without a control channel slight modifications were made. A Ø5 mm through hole was punched in the pump chamber of the flow layer. This allowed the flow channel to also serve as a spacer layer. A PDMS diaphragm (~40 μm thick) was bonded to the side with no flow channels to serve as the deflecting diaphragm. Lastly, the drug reservoir was bonded to the flow channel to complete the drug delivery micropump.

5% v/v Tween-20 solution was used in previous characterization experiments to minimize PS microsphere adsorption in the check valve and micropump; however Tween-20 significantly increases the solubility of DTX such that a constant drug concentration in the reservoir can no longer be guaranteed. BSA in PBS solution is considered an appropriate substitute for physiological fluid. An experiment showed that flushing 1% (w/v) BSA+PBS into the microfluidic device and left for 10 minutes was able to prevent PS microspheres from adsorbing onto the PDMS surface. Therefore, the trial drug diffusion study used 1% BSA+PBS as a substitute for Tween-20. It should be noted that DTX has a solubility limit of about 5-7 μg mL^{-1} in 1% BSA+PBS [21]; therefore the 100 μg DTX in the drug reservoir capable of delivering a maximum volume of 20 mL of DTX at its maximum solubility limit.

A standard linear curve relating the amount of DTX drug to a measured value of DPM is shown in Figure 4.3. Therefore, DPM readings of solutions from actuation and diffusion

experiments can be related to the amount of DTX released. Diffusion comparison between a micropump with microsphere in the check valve chamber versus a micropump with no microspheres was conducted and the results are shown in Figure 4.4. In contrast, the micropump with microspheres in the valve chamber was manually actuated once using a 3 mm diameter 1.26 g cylinder translating to a pressure of ~ 1.75 kPa and plotted alongside the diffusion values.

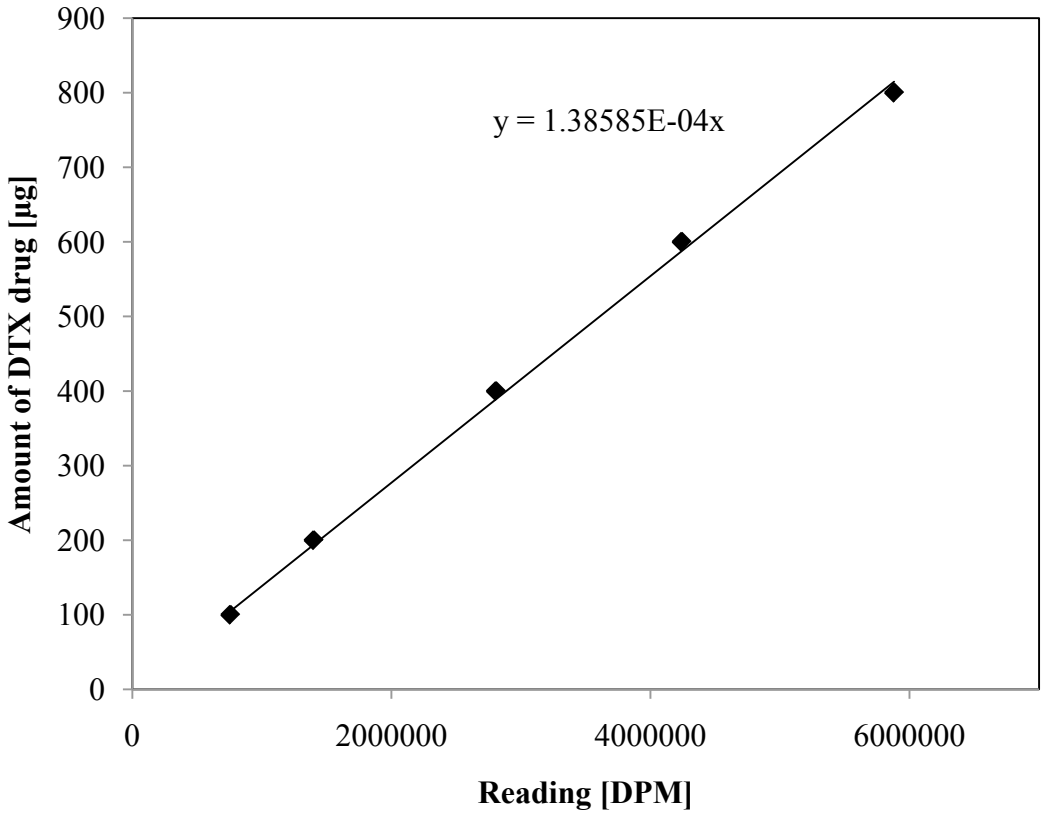

Figure 4.3 Standard curve relating the amount of DTX drug to the disintegrations per minute measurement (DPM) value.

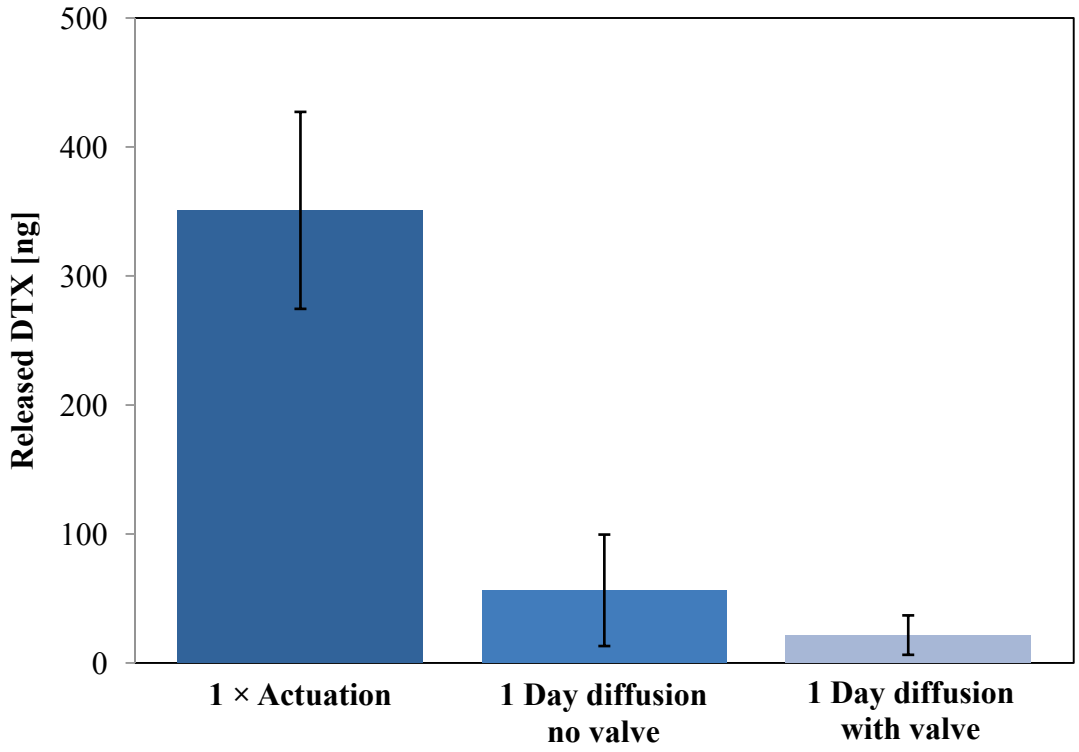

Figure 4.4 DTX released through actuation and diffusion from device with valves and without valves. Error bars represent one standard deviation from the mean (n=3).

Figure 4.4 shows a single actuation of 1.75 kPa released 350.84 ng of DTX. The average daily diffusion from the micropump with no microspheres in the valve chamber was 56.32 ng. However, the average diffusion from the micropump with microspheres in the valve chamber was 21.60 ng, representing a 62% reduction compared to the device with no microspheres.

The trial study shows that the microsphere check valve was effective in limiting diffusion from the micropump. Although the results are promising, further studies are required to investigate the performance of the proposed micropump as a drug delivery system.

Chapter 5: **Conclusions and future work**

5.1 Conclusion

The work presented in this thesis demonstrated the use of microspheres as fluid resistance elements in low pressure and low flow rate pumping. We have demonstrated the design, fabrication and characterization of a microfluidic check valve and the integration of such check valves in a planar micropump. The check valve and micropump were fabricated using standard soft lithography and injecting microspheres into the valve chamber. The microvalve satisfied the structurally thin physical requirement by having a flow channel 35 μm in height and using Ø20 μm PS microspheres.

The check valve was tested between 200 Pa and 3000 Pa and the 250-2000 μm valve achieved a maximum diodicity of 18. The 250-500 μm, 500-1000 μm and 250-1000 μm check valves achieved experimental diodicity of 3.7, 3.3 and 13.4, respectively, which is a considerable improvement over previous work. Other existing check valves do not exhibit as high diodicity in low pressure and low flow applications. In addition, the results suggests that increasing the porous media lengths in the check valves by increasing the number of microspheres may allow the check valve to perform to their theoretical diodicity. The new check valve concept using microspheres as fluid resistance elements represents advancement towards a feasible solution to micropumps with low actuation forces.

The micropump was delivered volumes between 0.26 μL and 1.26 μL per stroke with applied pressures between 200 Pa and 1000 Pa, which are suitable volumes for ocular drug delivery

applications since they are within the physiological fluid volume range found in the eye. Furthermore, a trial drug diffusion study showed the micropump's ability to limit diffusion from the drug reservoir. This was attributed to the increased tortuosity in the porous media formed by microspheres in the check valve.

5.2 Recommendation for future work

The micropump used in the volume flow characterization and trial drug study required a spacer layer to prevent the flexible diaphragm from bonding to other PDMS surfaces during fabrication. A multilayer mold could be fabricated to allow adequate clearance between the diaphragm and other PDMS surfaces eliminating the need of a spacer layer. Research can be done to develop the fabrication process to integrate a magnetic diaphragm and make the PDMS layers thin so that the overall thickness of the micropump falls within the 300-500 μm design requirement.

The current check valve design shows the possibility of achieving high diodicity under low pressure and low flow rates. However, the lower than expected diodicity suggests the Blake-Kozeny equation is not sufficient in predicting the diodicity of the check valve due to the inconsistent porosity in the porous media. More work can be done to study the porosity of the porous media formed in the valve chamber to better model the check valve diodicity based on the flow rate, and porous media length. A better understanding of the check valve's diodicity will allow for better control over volumes delivered by the micropump.

Another area of future research is to study the performance reliability of the check valve. Tween-20 and BSA+PBS solutions were used as surfactants to prevent the PS microspheres

from adsorbing to the PDMS. During flow measurements some microspheres managed to adsorb onto the PDMS surface and some at the retaining pillars over time, which can cause changes to system performance. Research can be conducted using microspheres made from different materials and/or have surface modifications to study whether they prevent the microspheres from adsorbing onto PDMS while using BSA+PBS as the working solution. Furthermore, a more reliable method of injecting and creating good sealing of microspheres in the valve chamber of the device can be developed. Research can be conducted to prove the robustness and reliability of the check valve.

References

[1] E. Verpoorte and N. F. De Rooij, "Microfluidics meets MEMS," *Proceedings of the Ieee,* vol. 91, pp. 930-953, Jun 2003.

[2] P.-A. Auroux*, et al.*, "Micro Total Analysis Systems. 2. Analytical Standard Operations and Applications," *Analytical Chemistry,* vol. 74, pp. 2637-2652, 2002.

[3] D. R. Reyes*, et al.*, "Micro Total Analysis Systems. 1. Introduction, Theory, and Technology," *Analytical Chemistry,* vol. 74, pp. 2623-2636, 2002.

[4] Y. Huang*, et al.*, "MEMS-based sample preparation for molecular diagnostics," *Analytical and Bioanalytical Chemistry,* vol. 372, pp. 49-65, Jan 2002.

[5] M. Toner and D. Irimia, "Blood-on-a-chip," in *Annual Review of Biomedical Engineering*. vol. 7, ed, 2005, pp. 77-103.

[6] P. S. Dittrich and A. Manz, "Lab-on-a-chip: microfluidics in drug discovery," *Nature Reviews Drug Discovery,* vol. 5, pp. 210-218, Mar 2006.

[7] L. Cao*, et al.*, "Design and simulation of an implantable medical drug delivery system using microelectromechanical systems technology," *Sensors and Actuators a-Physical,* vol. 94, pp. 117-125, Oct 31 2001.

[8] T. Bourouina*, et al.*, "Design and simulation of an electrostatic micropump for drug-delivery applications," *Journal of Micromechanics and Microengineering,* vol. 7, pp. 186-188, Sep 1997.

[9] N.-C. Tsai and C.-Y. Sue, "Review of MEMS-based drug delivery and dosing systems," *Sensors and Actuators A: Physical,* vol. 134, pp. 555-564, 2007.

[10] J. C. Lang, "Ocular drug delivery conventional ocular formulations," *Advanced Drug Delivery Reviews,* vol. 16, pp. 39-43, 1995.

[11] D. Ghate and H. F. Edelhauser, "Barriers to glaucoma drug delivery," *Journal of Glaucoma,* vol. 17, pp. 147-156, Mar 2008.

[12] L. Van Santvliet and A. Ludwig, "Determinants of eye drop size," *Survey of Ophthalmology,* vol. 49, pp. 197-213, Mar-Apr 2004.

[13] S. Mishima*, et al.*, "Determination of tear volume and tear flow," *Investigative ophthalmology,* vol. 5, pp. 264-76, 1966-Jun 1966.

[14] R. Lo*, et al.*, "A passive MEMS drug delivery pump for treatment of ocular diseases," *Biomedical Microdevices,* vol. 11, pp. 959-970, 2009.

[15] R. Lo*, et al.*, "A refillable microfabricated drug delivery device for treatment of ocular diseases," *Lab on a chip,* vol. 8, pp. 1027-1030, 2008.

[16] C.-P.-B. Siu and M. Chiao, "A Microfabricated PDMS Microbial Fuel Cell," *Journal of Microelectromechanical Systems,* vol. 17, pp. 1329-1341, Dec 2008.

[17] S. Choi*, et al.*, "A [small mu]L-scale micromachined microbial fuel cell having high power density," *Lab on a chip,* vol. 11, pp. 1110-1117, 2011.

[18] F. Qian*, et al.*, "A 1.5 [small micro]L microbial fuel cell for on-chip bioelectricity generation," *Lab on a chip,* vol. 9, pp. 3076-3081, 2009.

[19] F. Albano, *et al.*, "A fully integrated microbattery for an implantable microelectromechanical system," *Journal of Power Sources,* vol. 185, pp. 1524-1532, Dec 1 2008.

[20] M. Khoo and C. Liu, "A novel micromachined magnetic membrane microfluid pump," in *Proceedings of the 22nd Annual International Conference of the Ieee Engineering in Medicine and Biology Society, Vols 1-4*. vol. 22, J. D. Enderle, Ed., ed, 2000, pp. 2394-2397.

[21] F. N. Pirmoradi, *et al.*, "On-demand controlled release of docetaxel from a battery-less MEMS drug delivery device," *Lab on a chip,* vol. 11, pp. 2744-52, 2011-Aug-21 2011.

[22] J. J. Nagel, *et al.*, "Magnetically actuated micropumps using an Fe-PDMS composite membrane - art. no. 617213," *Smart Structures and Materials 2006: Smart Electronics, Mems, Biomems, and Nanotechnology,* vol. 6172, pp. 17213-17213, 2006.

[23] F. Pirmoradi, *et al.*, "A magnetic poly(dimethylesiloxane) composite membrane incorporated with uniformly dispersed, coated iron oxide nanoparticles," *Journal of Micromechanics and Microengineering,* vol. 20, Jan 2010.

[24] N. L. Jeon, *et al.*, "Microfluidics Section: Design and Fabrication of Integrated Passive Valves and Pumps for Flexible Polymer 3-Dimensional Microfluidic Systems," *Biomedical Microdevices,* vol. 4, pp. 117-121, 2002.

[25] K. W. Oh and C. H. Ahn, "A review of microvalves," *Journal of Micromechanics and Microengineering,* vol. 16, pp. R13-R39, May 2006.

[26] J. Loverich, *et al.*, "Single-step replicable microfluidic check valve for rectifying and sensing low Reynolds number flow," *Microfluidics and Nanofluidics,* vol. 3, pp. 427-435, 2007.

[27] B. Z. Yang and Q. Lin, "Planar micro-check valves exploiting large polymer compliance," *Sensors and Actuators a-Physical,* vol. 134, pp. 186-193, 2007.

[28] J. J. Loverich, *et al.*, "Concepts for a new class of all-polymer micropumps," *Lab on a chip,* vol. 6, pp. 1147-1154, 2006.

[29] E. Stemme and G. Stemme, "A Valveless Diffuser/Nozzle-Based Fluid Pump," *Sensors and Actuators a-Physical,* vol. 39, pp. 159-167, Nov 1993.

[30] K. S. Yang, *et al.*, "Novel no-moving-part valves for microfluidic devices," *Microsystem Technologies-Micro-and Nanosystems-Information Storage and Processing Systems,* vol. 16, pp. 1691-1697, Oct 2010.

[31] T. R. Pan, *et al.*, "A magnetically driven PDMS micropump with ball check-valves," *Journal of Micromechanics and Microengineering,* vol. 15, pp. 1021-1026, 2005.

[32] M. Shen, *et al.*, "Miniaturized PMMA ball-valve micropump with cylindrical electromagnetic actuator," *Microelectronic Engineering,* vol. 85, pp. 1104-1107, 2008.

[33] (Patient UK (n.d)), *Allergic Conjunctivitis*. Available: http://www.patient.co.uk/health/Allergic-Conjunctivitis.htm

[34] J. R. C. H. Gebhard, UT, US), Patel, Dinesh (Salt Lake City, UT, US), "TAXANE COMPOUNDS FOR TREATING EYE DISEASE," United States Patent, 2011.

[35] F. N. Pirmoradi*, et al.*, "A Magnetically Controlled MEMS Device for Drug Delivery: Design, Fabrication, and Testing," *Lab on a chip,* In press.

[36] J. P. Abulencia and L. Theodore, *Fluid flow for the practicing chemical engineer*. Hoboken, N.J.: John Wiley & Sons, 2009.

[37] G. M. Whitesides*, et al.*, "Soft lithography in biology and biochemistry," *Annual Review of Biomedical Engineering,* vol. 3, pp. 335-373, 2001 2001.

[38] J. C. McDonald and G. M. Whitesides, "Poly(dimethylsiloxane) as a material for fabricating microfluidic devices," *Accounts of Chemical Research,* vol. 35, pp. 491-499, Jul 2002.

[39] M. C. Belanger and Y. Marois, "Hemocompatibility, biocompatibility, inflammatory and in vivo studies of primary reference materials low-density polyethylene and polydimethylsiloxane: A review," *Journal of Biomedical Materials Research,* vol. 58, pp. 467-477, Oct 2001.

[40] M. L. Aguiar and J. R. Coury, "Cake formation in fabric filtration of gases," *Industrial & Engineering Chemistry Research,* vol. 35, pp. 3673-3679, Oct 1996.

[41] A. Y. Al-Otoom, "Prediction of the collection efficiency, the porosity, and the pressure drop across filter cakes in particulate air filtration," *Atmospheric Environment,* vol. 39, pp. 51-57, Jan 2005.

[42] W. M. Lu and K. J. Hwang, "Mechanism of Cake Formation in Constant-Pressure Filtrations," *Separations Technology,* vol. 3, pp. 122-132, Jul 1993.

[43] Y.-S. Yu and Y.-P. Zhao, "Deformation of PDMS membrane and microcantilever by a water droplet: Comparison between Mooney-Rivlin and linear elastic constitutive models," *Journal of Colloid and Interface Science,* vol. 332, pp. 467-476, Apr 15 2009.

[44] L. Shen and Z. X. Chen, "Critical review of the impact of tortuosity on diffusion," *Chemical Engineering Science,* vol. 62, pp. 3748-3755, Jul 2007.

Appendices

Appendix A Detailed drawings of check valves

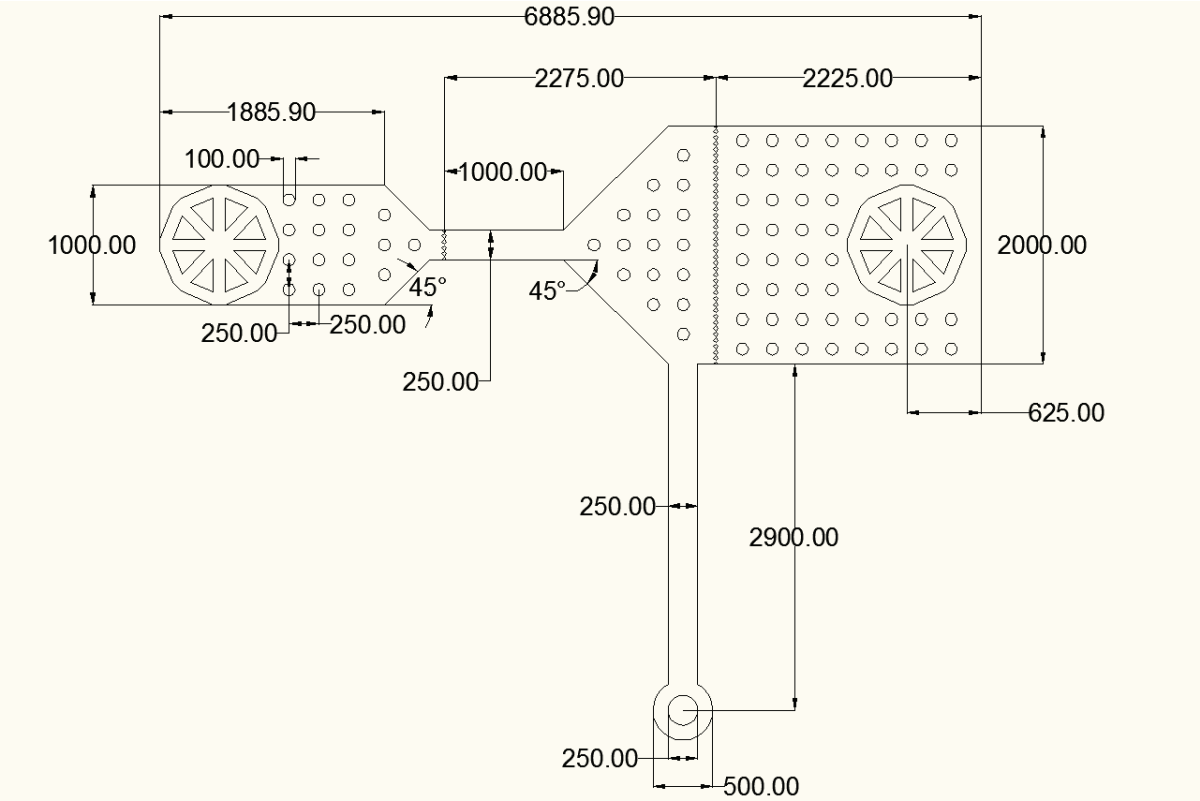

Figure A.1 Detailed drawing of 250-2000 µm check valve (dimensions in µm).

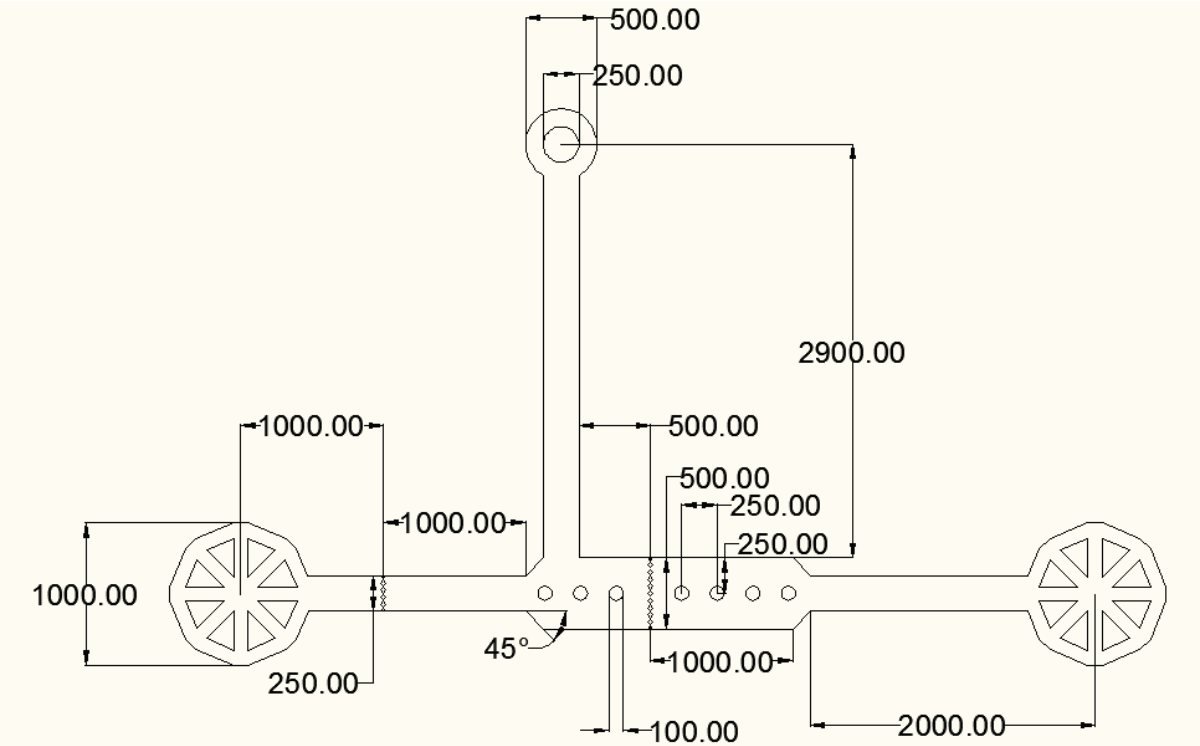

Figure A.2 Detailed drawing of 250-500 µm check valve (dimensions in µm).

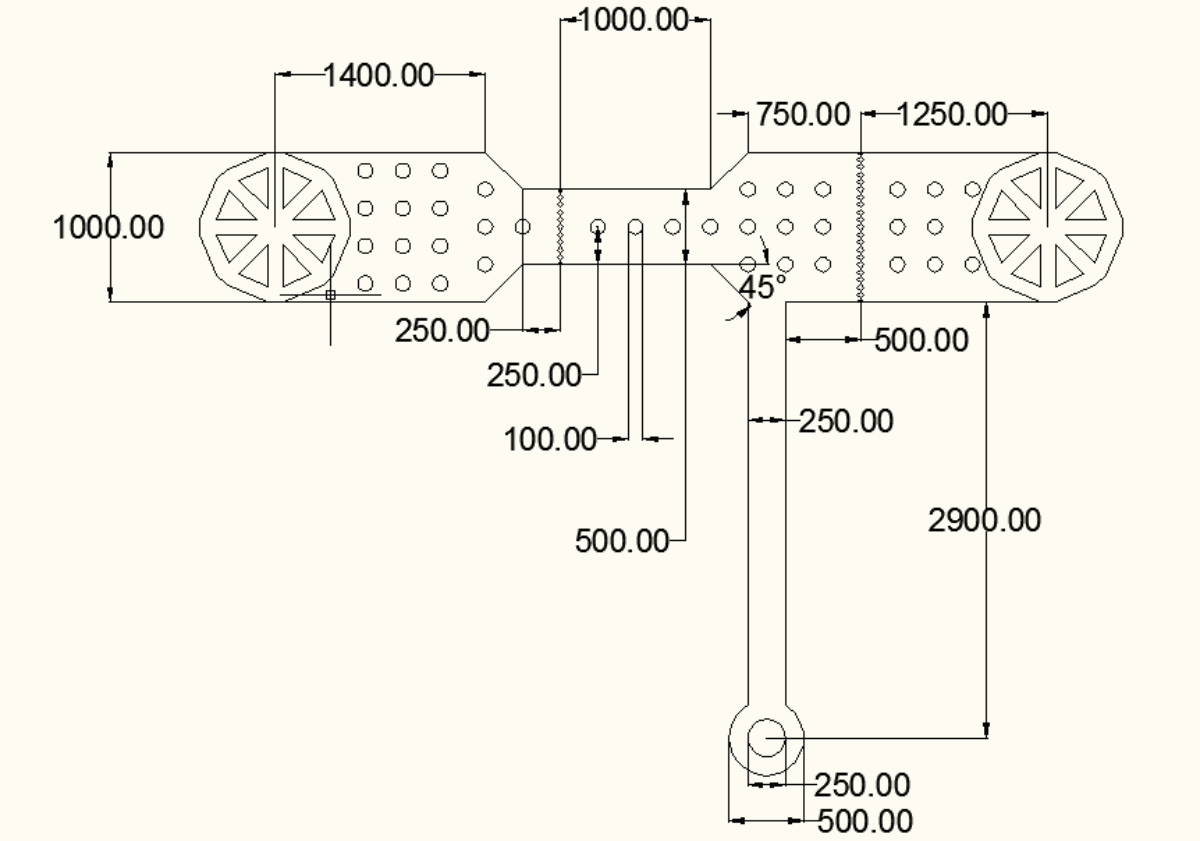

Figure A.3 Detailed drawing of 500-1000 µm check valve (dimensions in µm).

Appendix B Characterization procedure

B.1 Check valve characterization procedure

1. Apply 100 Pa to both pressurized fluid reservoirs to fill tubing with 5% v/v Tween-20 solution. Make sure no air bubbles are present in the tubing.

2. Connect the fluid tubing from flow sensor 1 to the microfluidic device by inserting the stainless steel tip into the inlet of check valve device.

3. Fill the microfluidic channel with 5% v/v Tween-20 solution.

4. Close off microsphere inlet channel by inserting blocked stainless steel tip.

5. Connect the fluid tubing from flow sensor 2 to the microfluidic device by inserting the stainless steel tip into the outlet of the check valve.

6. Degas the microfluidic channel by pressurizing the system from 0.1 to 30 kPa at 0.5 kPa increments in 5 second intervals. This is done by increasing the pressures in both fluid reservoirs simultaneously.

7. When gas bubbles are gone, de-pressurize the system from 30 kPa to 0.1 kPa at 0.5 kPa decrements in 5 second intervals.

8. Remove blocked stainless steel pin and inject microspheres into the microsphere inlet channel using syringe or pressurized fluid reservoir with microsphere solution. When the desired amount of microspheres is in the channel, insert the blocked stainless steel tip to close off the microsphere inlet channel. The microspheres will be trapped in the valve chamber by the PDMS pillars.

9. Repeat steps 6 and 7 to degas the system.

10. Apply a base pressure of 10kPa in both pressurized fluid reservoirs. A base pressure enables the MFCS to apply pressure differences more precisely. The base pressure introduces hydrostatic pressure in the device; however the support pillars and narrow channel widths prevent the microfluidic channel from expanding. Test experiments with 0 kPa base pressure resulted in flow rates differences <5% from the flow measurements using 10 kPa base pressure.

11. Run the MAESFLOW script which increases the pressure difference at the programmed increments. The flow measurements are conducted in one direction only (reverse or forward). The applied pressure is held for 10 seconds and a recording script records the flow rate and actual pressures applied. Inject microspheres into microsphere inlet channel.

12. Remove and insert the inlet tubing for the opposite direction test. (i.e. insert the fluid tubing from sensor 1 into the outlet of the check valve and insert fluid tubing from sensor 2 to the inlet of the check valve) NOTE: for characterizing the check valve in oscillating flow, this step is skipped since the oscillating flow is controlled by the MAESFLOW script

13. Measure flow rates in the opposite direction by repeating step 11.

B.2 Micropump characterization procedure

1. Fill the flow channel and control channel of the micropump by injecting 5% v/v Tween-20 solution using a syringe or pressurized fluid reservoir.

2. Place micropump in beaker with 5% v/v Tween-20 solution.

3. Place beaker with micropump in a vacuum desiccator to remove large air bubbles.

4. Place beaker with micropump in the fridge at ~4°C for a minimum of 12 hours to allow air bubbles to diffuse out of the micropump.

5. When gas bubbles are removed from the system, inject microspheres into the microsphere inlet channel using a syringe or pressurized fluid. When the desired amount of microspheres is in the channel, insert the blocked stainless steel tip to close off the microsphere inlet channel. The microspheres will be trapped in the valve chamber by the PDMS pillars. This step is performed for the check valve on the inlet side of the pump chamber and on the outlet side of the pump chamber.

6. Apply 100 Pa to both pressurized fluid reservoirs to fill tubing with 5% v/v Tween-20 solution. Make sure no air bubbles are present in the tubing.

7. Connect the fluid tubing from flow sensor 1 and flow sensor 2 to the micropump by inserting the stainless steel tip into the inlet and outlet of the micropump. The flow sensors are connected to fluid reservoirs which are not pressurized.

8. Connect the fluid tubing from the pressurized fluid reservoir to the control channel inlet.

9. Run the MAESFLOW script which increases the pressure in the pressurized fluid reservoir at the programmed increments. Run the Labview program which controls the cycle time and duty cycle of the solenoid valve. Each applied pressure cycle is

performed 3 times. A recording script records the flow rates from the inlet and outlet of the micropump

Appendix C Supplemental check valve characterization data

C.1 Characterization of 250-500 µm check valve

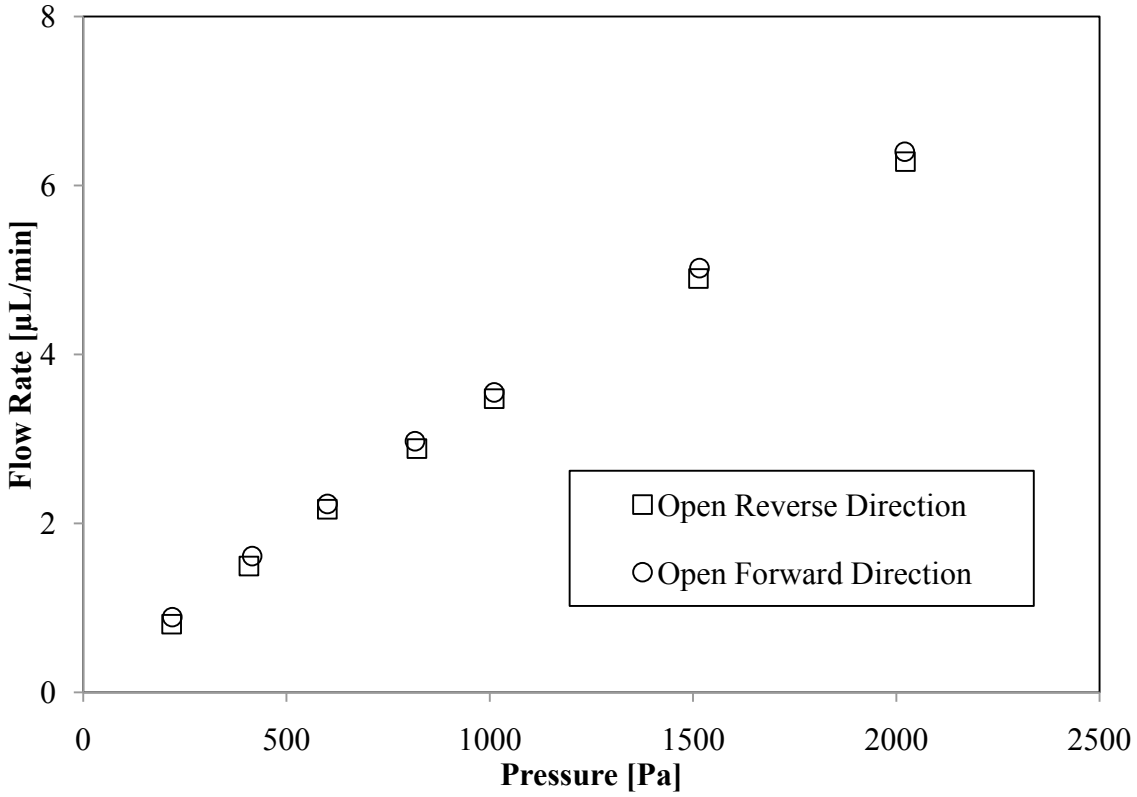

Figure C.1 Flow rate of valve channel with no microspheres for 250-500 µm check valve.

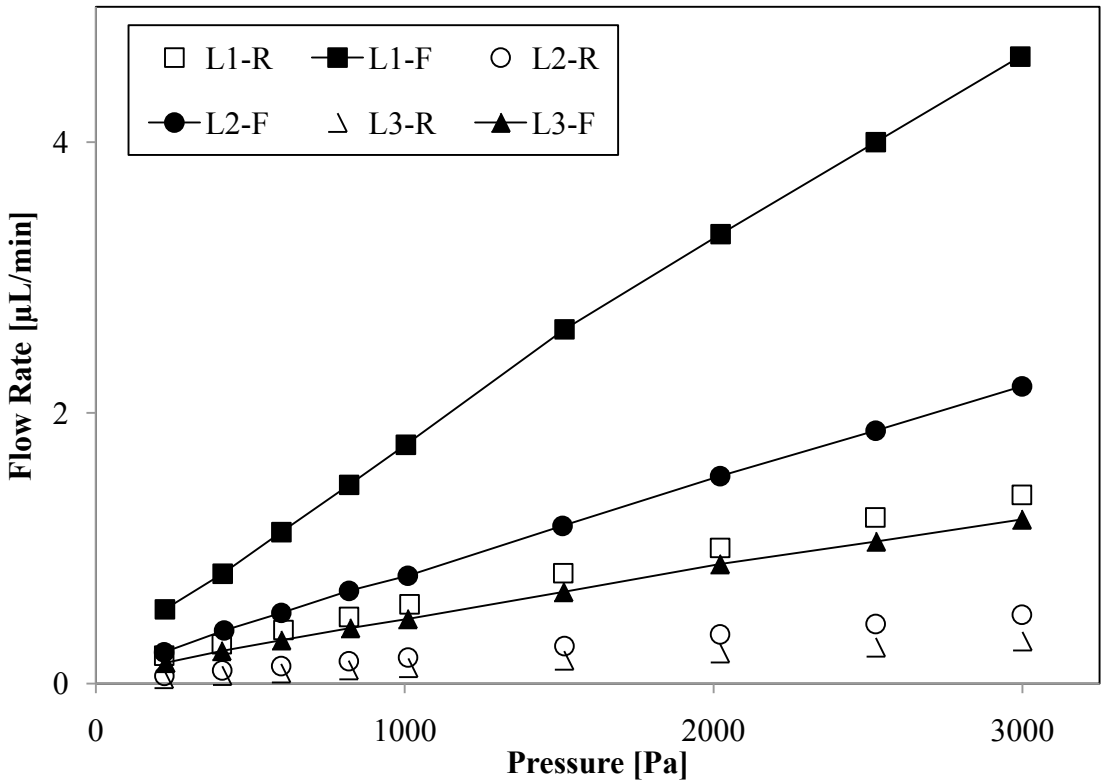

Figure C.2 Flow rate versus pressure difference at porous lengths L1-L3 (see Table 3.1) for 250-500 µm check valve.

C.2 Characterization of 500-1000 µm check valve

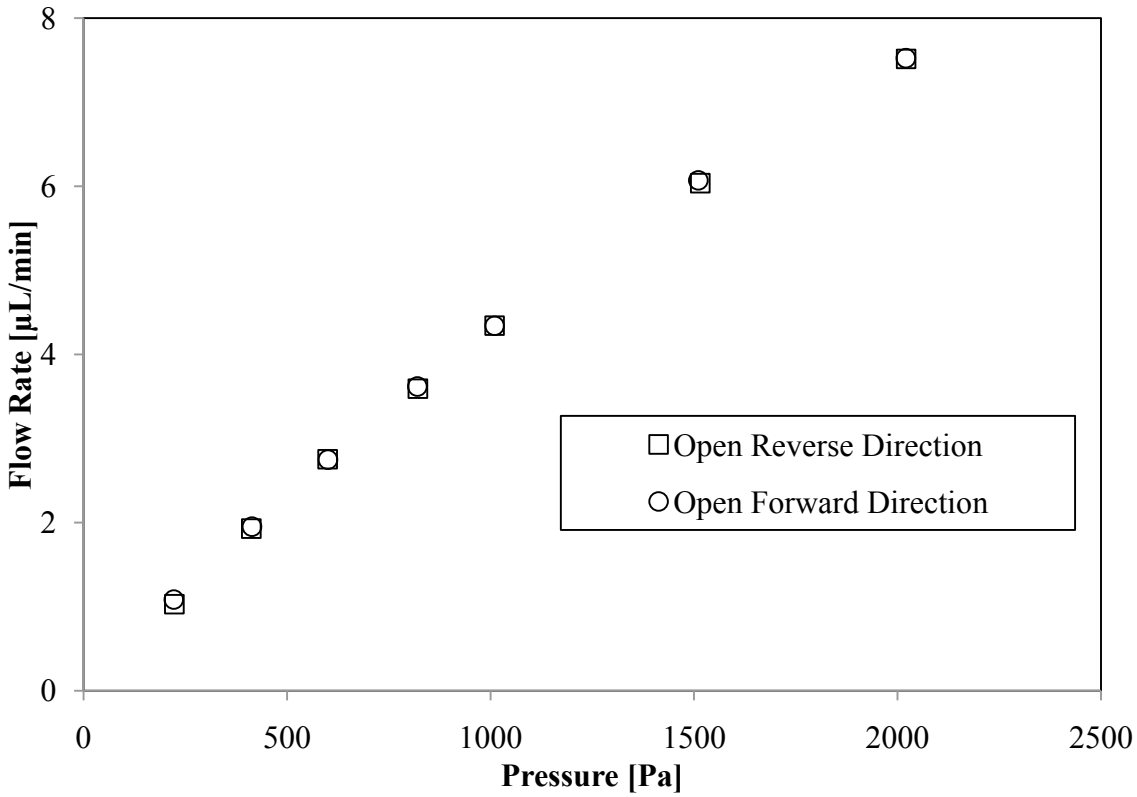

Figure C.3 Flow rate of valve channel with no microspheres for 500-1000 µm check valve.

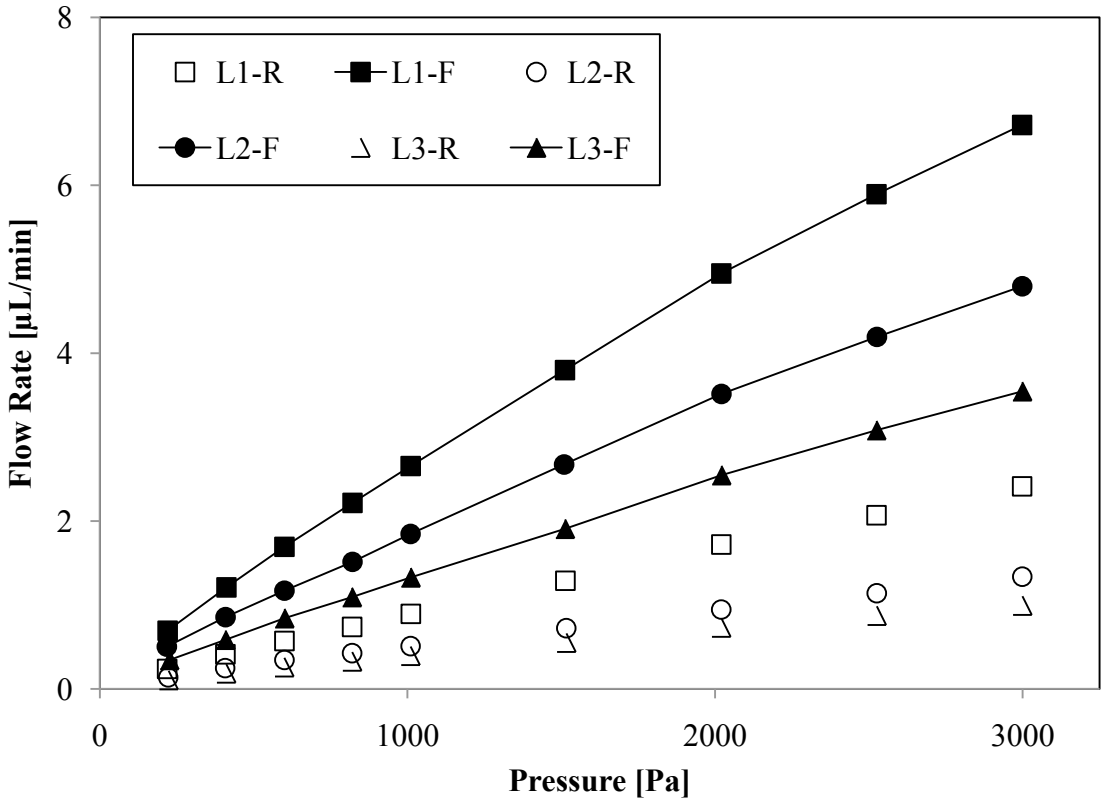

Figure C.4 Flow rate versus pressure difference at porous lengths L1-L3 (see Table 3.1) for 500-1000 µm check valve.

Appendix D Volume flow from micropump based on cycle time

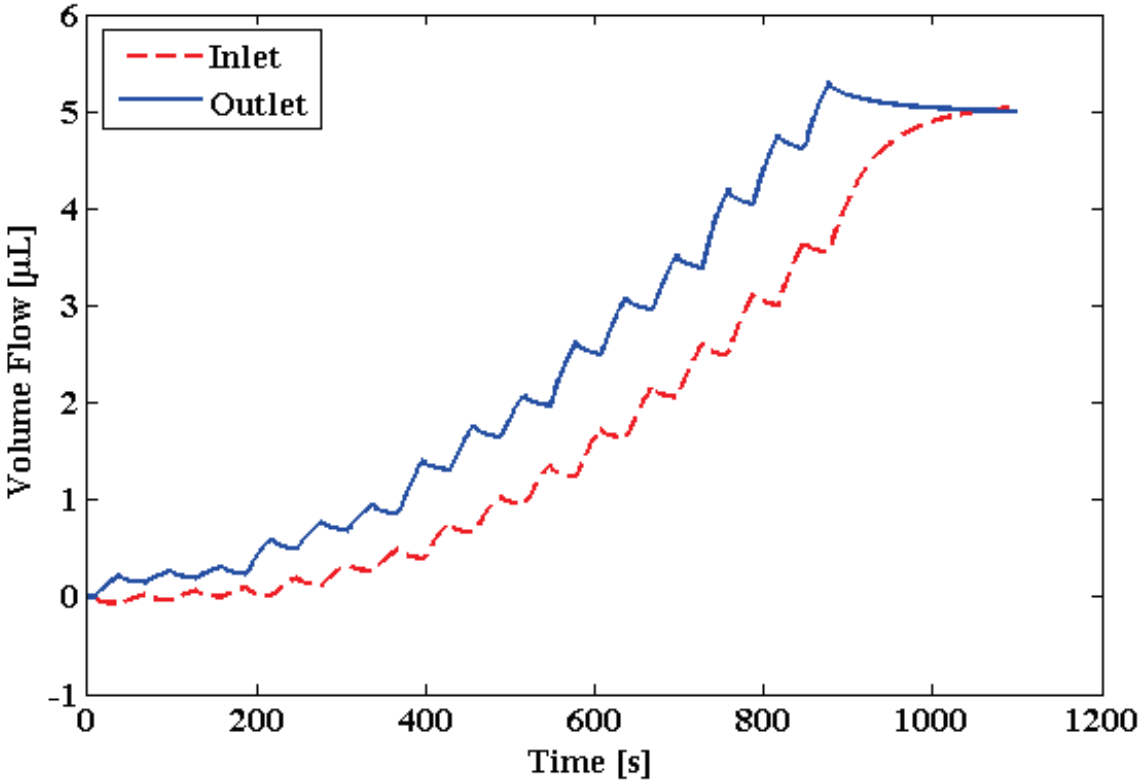

Figure D.1 Volume flow measurement of the micropump with 60 seconds cycle time and 50% duty cycle

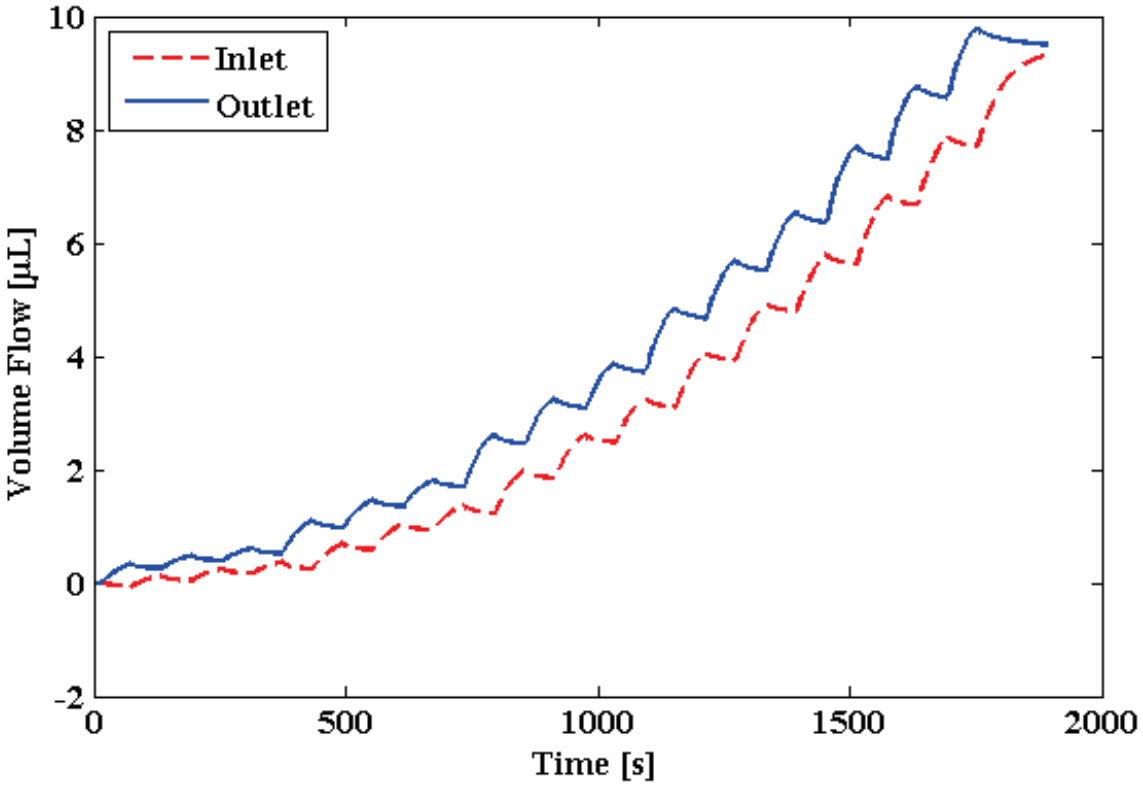

Figure D.2 Volume flow measurement of the micropump with 120 seconds cycle time and 50% duty cycle